

# A Robust Optimization Approach to Deep Learning

**Dimitris Bertsimas**

*Sloan School of Management and Operations Research Center  
Massachusetts Institute of Technology  
Cambridge, MA 02139, USA*

DBERTSIM@MIT.EDU

**Xavier Boix**

*Department of Brain and Cognitive Sciences  
Massachusetts Institute of Technology  
Cambridge, MA 02139, USA*

XBOIX@MIT.EDU

**Kimberly Villalobos Carballo**

*Operations Research Center  
Massachusetts Institute of Technology  
Cambridge, MA 02139, USA*

KIMVC@MIT.EDU

**Dick den Hertog**

*Amsterdam Business School  
University of Amsterdam  
Plantage Muidersgracht 12, 1018 TV Amsterdam, The Netherlands*

D.DENHERTOG@UVA.NL

## Abstract

Many state-of-the-art adversarial training methods leverage upper bounds of the adversarial loss to provide security guarantees. Yet, these methods require computations at each training step that can not be incorporated in the gradient for backpropagation. We introduce a new, more principled approach to adversarial training based on a closed form solution of an upper bound of the adversarial loss, which can be effectively trained with backpropagation. This bound is facilitated by state-of-the-art tools from robust optimization. We derive two new methods with our approach. The first method (*Approximated Robust Upper Bound* or aRUB) uses the first order approximation of the network as well as basic tools from linear robust optimization to obtain an approximate upper bound of the adversarial loss that can be easily implemented. The second method (*Robust Upper Bound* or RUB), computes an exact upper bound of the adversarial loss. Across a variety of tabular and vision data sets we demonstrate the effectiveness of our more principled approach —RUB is substantially more robust than state-of-the-art methods for larger perturbations, while aRUB matches the performance of state-of-the-art methods for small perturbations. Also, both RUB and aRUB run faster than standard adversarial training (at the expense of an increase in memory). All the code to reproduce the results can be found at <https://github.com/kimvc7/Robustness>.

**Keywords:** deep learning, optimization, robustness

## 1. Introduction

Robustness of neural networks for classification problems has received increasing attention in the past few years, since it was exposed that these models could be easily fooled by introducing some small perturbation in the input data. These perturbed inputs, which are commonly referred to as *adversarial examples*, are visually indistinguishable from the natural input, and neural networks simply trained to maximize accuracy often assign them to an incorrect class (Szegedy et al., 2013). This problem becomes particularly relevant when considering applications related to self-driving cars or medicine, in which adversarial examples represent an important security threat (Kurakin et al., 2016).

The Machine Learning community has recently developed multiple heuristics to make neural networks robust. The most popular ones are perhaps those based on adversarial training, a method first proposed by Goodfellow et al. (2015) and which consists in training the neural network using adversarial inputs instead of the standard data. The defense by Madry et al. (2019), which finds the adversarial examples with bounded norm using iterative projected gradient descent (PGD) with random starting points, has proved to be one of the most effective methods (Tjeng et al., 2019). Other heuristic defenses rely on preprocessing or projecting the input space (Lamb et al., 2018; Kabilan et al., 2018; Ilyas et al., 2017), on randomizing the neurons (Prakash et al., 2018; Xie et al., 2017) or on adding a regularization term to the objective function (Ross and Doshi-Velez, 2017; Hein and Andriushchenko, 2017; Yan et al., 2018). There is a plethora of heuristics for adversarial robustness by now. Yet, these defenses are only effective to adversarial attacks of small magnitude and are vulnerable to attacks of larger magnitude or to new attacks (Athalye et al., 2018).

A recent strand of research has been to leverage upper bounds of the adversarial loss to improve adversarial robustness. These upper bounds provide security guarantees against adversarial attacks, even new ones, by finding a mathematical proof that a network is not susceptible to any attack, e.g. (Dathathri et al., 2020; Raghunathan et al., 2018b; Katz et al., 2017; Tjeng et al., 2019; Bunel et al., 2017; Anderson et al., 2020; Singh et al., 2018; Zhang et al., 2018; Weng et al., 2018; Gehr et al., 2018; Dvijotham et al., 2018b; Lecuyer et al., 2019; Cohen et al., 2019). The upper bounds have also been incorporated in the training of adversarial defenses. Wong and Kolter (2018) for instance, find an upper bound for the adversarial loss by considering the polytope generated by adversarial examples with bounded norm and minimizing the loss over a convex polytope that contains it. An upper bound on the adversarial loss is also computed in Raghunathan et al. (2018a) by solving instead a semidefinite program. Other more scalable and effective methods based on minimizing an upper bound of the adversarial loss have been introduced (Gowal et al., 2019; Balunovic and Vechev, 2019; Mirman et al., 2018; Dvijotham et al., 2018a; Wong et al., 2018; Zhang et al., 2019).

While these methods provide security guarantees, most of them require complex intermediate computations that depend on the training parameters of the network and can not be incorporated in the gradient for backpropagation. Since the direction of the gradient is then not precise, the optimization process may be problematic. Even though a couple of these approaches do provide an upper bound with closed form solution (Raghunathan et al., 2018a; Gowal et al., 2019), they only work for specific cases (Raghunathan et al. (2018a) only works for neural networks with two layers, and the upper bound in Gowal et al. (2019) is often loose and it only applies when the perturbations are in the  $L_\infty$  norm-bounded ball). Given this state of affairs, we believe we need a new, principled approach to optimize an upper bound of the adversarial loss.

A promising approach that has not been comprehensively explored is the usage of state-of-the-art robust optimization tools (Bertsimas and den Hertog, 2022). Robust optimization has been tremendously effective to solve optimization problems with uncertainty in the parameters, which may arise from rounding or implementation errors. It provides guarantees to uncertainty in the parameters of the model and could be leveraged for deep learning (Bertsimas et al., 2019). In this paper, we use state-of-the-art robust optimization tools to derive a new closed form solution of an upper bound of the adversarial loss. This leads to a more principled approach to adversarial training that can be effectively trained with backpropagation.

We develop two new methods for training deep learning models that are robust against input perturbations. The first method (*Approximated Robust Upper Bound* or aRUB), minimizes an approximated upper bound of the robust loss for  $L_p$  norm bounded uncertainty sets, for general  $p$ . It is simple to implement and performs similarly to adversarial training on small uncertainty sets while running significantly faster. The second method (*Robust Upper Bound* or RUB), minimizes an exact upper bound of the robust loss specifically for  $L_1$  norm bounded uncertainty sets. This method shows the best performance for larger uncertainty sets and also runs faster than adversarial training. More importantly, it provides security guarantees against  $L_1$  norm bounded adversarial attacks. Lastly, we show that robust training can significantly improve the natural accuracy compared to standard non-robust training methods. More concretely, we introduce the following robustness methods:

- *Approximated Robust Upper Bound* or aRUB: We develop a simple method to approximate an upper bound of the robust problem by adding a regularization term for each class separately. As an alternative to standard adversarial training (which relies on linear approximations to find good adversarial attacks), we use the first order approximation of the network to estimate the worst case scenario for each individual class. We then apply standard results from linear robust optimization to obtain a new objective that behaves like an upper bound of the robust loss and which can be tractably minimized for robust training. This method can be easily implemented and performs very well when the uncertainty set radius  $\rho$  is small. It has a higher memory requirement than nominal training, but it significantly reduces training time compared to other robust methods like adversarial training.
- *Robust Upper Bound* or RUB: We extended state-of-the-art tools from robust optimization to function that like neural networks are neither convex nor concave. By splitting each layer of the network as the sum of a convex function and a concave function, we are able to obtain an exact upper bound of the robust loss for the case in which the uncertainty set is the  $L_1$  sphere. Since the dual function of the  $L_1$  norm is the  $L_\infty$  norm, we convert the maximum over the uncertainty set into a maximum over a finite set. In the end, instead of minimizing the worst case loss over an infinite uncertainty set, the new objective minimizes the worst case loss over a discrete set whose cardinality is twice the dimension of the input data. While this represents a significant increase in memory for high dimensional inputs, we show that this approach remains tractable for multiple applications. In addition, this methods allows for parallelization and the overall computational time is much lower than the one achieved with other algorithms like adversarial training. The main advantage of this method is that it provides security guarantees against adversarial examples bounded in the  $L_1$  norm. Additionally, we also show experimentally that this method generally achieves the highest adversarial accuracies for larger uncertainty sets.

Also, we show that these methods consistently achieve higher standard accuracy (i.e., non adversarial accuracy), than the nominal neural networks trained without robustness. While this result is not true for a general choice of uncertainty set (see for example Ilyas et al. (2019)), we observe that when the uncertainty set has the appropriate size it can significantly improve the classification performance of the network, which is consistent with the results obtained for other classification models like Support Vector Machines, Logistic Regression and Classification Trees (Bertsimas et al., 2019).

The paper is organized as follows: Section 2 revisits related work with robust Optimization and deep learning, Section 3 defines the robust problem, Section 4 presents our first method (Approximate Robust Upper Bound), and Section 5 contains our second method (Robust Upper Bound). Lastly, Section 6 contains the results for the computational experiments.

## 2. Previous Works on Robust Optimization

Over the last two decades, robust optimization has become a successful approach to solve optimization problems under uncertainty. For an overview of the primary research in this field we refer the reader to Bertsimas et al. (2011). Areas like mathematical programming and engineering have long applied these tools to develop models that are robust against uncertainty in the parameters, which may arise from rounding or implementation errors. For many applications, the robust problem can be reformulated as a tractable optimization problem, which is referred to as the *robust counterpart*. For instance, for several types of uncertainty sets, the robust counterpart of a linear programming problem can be written as a linear or conic programming problem (Ben-Tal et al., 2009), which can be solved with many of the current optimization software. While there is not a systematic way to find robust counterparts for a general nonlinear uncertain problem, multiple techniques have been developed to obtain tractable formulations in some specific nonlinear cases.

As shown in Ben-Tal et al. (2009), the exact robust counterpart is known for Conic Quadratic Problems and Semidefinite problems in which the uncertainty is finite, an interval or an unstructured norm-bounded set. More generally, it is shown in Ben-Tal et al. (2015) that for problems in which the objective function or the constraints are concave in the uncertainty parameters, Fenchel duality can be used to exactly derive the corresponding robust counterpart. While the result does not necessarily have a closed form, the authors show that it yields a tractable formulation for the most common uncertainty sets (e.g. polyhedral and ellipsoidal uncertainty sets).

The problem becomes significantly more complex when the functions in the objective or in the constraints are instead convex in the uncertainty (Chassein and Goerigk, 2019). Since obtaining exact robust counterparts in these cases is generally infeasible, safe approximations are considered instead (Bertsimas et al., 2020). For instance, Zhen et al. (2017) develop safe approximations for the specific cases of second order cone and semidefinite programming constraints with polyhedral uncertainty. These techniques are generalized in Roos et al. (2020), where the authors convert the robust counterpart to an adjustable robust optimization problem that produces a safe approximation for any problem that is convex in the optimization variables as well as in the the uncertain parameters.

Even though the approaches mentioned above consider uncertainty in the parameters of the model as opposed to uncertainty in the input data, the same techniques can be utilized for obtaining

robust counterparts in the latter case. In fact, the robust optimization methodologies have recently been applied to develop machine learning models that are robust against perturbations in the input data. In Bertsimas et al. (2019), for example, the authors consider uncertainty in the data features as well as in the data labels to obtain tractable robust counterparts for some of the major classification methods: support vector machines, logistic regression, and decision trees. However, due to the high complexity of neural networks as well as the large dimensions of the problems in which they are often utilized, robust counterparts or safe approximations for this type of models have not yet been developed. There are two major challenges with applying robust optimization tools for training robust neural networks:

- (i) *Neural networks are neither convex nor concave functions:* As mentioned earlier, robust counterparts are difficult to find for a general problem. Although plenty of work has been done to find tractable reformulations as well as safe approximations, all of them rely on the underlying function being a convex or a concave function of the uncertainty parameters. Unfortunately, neural networks don't satisfy either condition, which makes it really difficult to apply any of the approaches discussed above.
- (ii) *The robust counterpart needs to preserve the scalability of the model:* Neural networks are most successful in problems involving vision data sets, which often imply large input dimensions and enormous amount of data. For the most part, they can still be successfully trained thanks to the fact that back propagation algorithms can be applied to solve the corresponding unconstrained optimization problem. However, the robust optimization techniques for both convex and concave cases often require the addition of new constraints and variables for each data sample, increasing significantly the number of parameters of the network and making it very difficult to use standard machine learning software for training.

A straightforward way to overcome both of these difficulties would be to replace the loss function of the network with its first order approximation. However, this loss function is usually highly nonlinear and therefore the linear approximation is very inaccurate. Our method aRUB explores a slight modification of this approach that significantly improves adversarial accuracy by considering only the linear approximation of the network's output layer.

Alternatively, a more rigorous approach to overcome problem (i) would be to piece-wise analyze the convexity of the network and apply the robust optimization techniques in each piece separately, but this approach would introduce additional variables that are in conflict with requirement (ii). For our RUB method we then develop a general framework to split the network by convexity type, and we show that in the specific case in which the uncertainty set is the  $L_1$  norm bounded sphere, we can solve for the extra variables and obtain an unconstrained problem that can be tractably solved using standard gradient descent techniques.

### 3. The Robust Optimization Problem

We consider a classification problem over data points  $\mathbf{x} \in \mathbb{R}^M$  with  $K$  different classes. Given weight matrices  $\mathbf{W}^\ell \in \mathbb{R}^{r_{\ell-1} \times r_\ell}$  and bias vectors  $\mathbf{b}^\ell \in \mathbb{R}^{r_\ell}$  for  $\ell \in [L]$ , such that  $r_0 = M, r_L = K$ , the corresponding feed forward neural network with  $L$  layers and ReLU activation function is

defined by the equations

$$\begin{aligned} \mathbf{z}^1(\theta, \mathbf{x}) &= \mathbf{W}^1 \mathbf{x} + \mathbf{b}^1, \\ \mathbf{z}^\ell(\theta, \mathbf{x}) &= \mathbf{W}^\ell [\mathbf{z}^{\ell-1}(\theta, \mathbf{x})]^+ + \mathbf{b}^\ell, \quad \forall 2 \leq \ell \leq L, \end{aligned}$$

where  $\theta$  denotes the set of parameters  $(\mathbf{W}^\ell, \mathbf{b}^\ell)$  for all  $\ell \in [L]$  and  $[\mathbf{x}]^+$  is the result of applying the ReLU function to each coordinate of  $\mathbf{x}$ . For fixed parameters  $\theta$ , the network assigns a sample  $\mathbf{x}$  to the class  $\hat{y} = \arg \max_k \mathbf{z}_k^L(\theta, \mathbf{x})$ . And given a data set  $\{(\mathbf{x}_n, y_n)\}_{n=1}^N$ , where  $y_n$  is the target class of  $\mathbf{x}_n$ , the optimal parameters  $\theta$  are usually found by minimizing the empirical loss

$$\min_{\theta} \frac{1}{N} \sum_{n=1}^N \mathcal{L}(y_n, \mathbf{z}^L(\theta, \mathbf{x}_n)), \quad (1)$$

with respect to a specific loss function  $\mathcal{L}$ .

In the robust optimization framework, however, we want to find the parameters  $\theta$  by minimizing the worst case loss achieved over an uncertainty set of the input. More specifically, instead of solving the nominal problem in Eq. (1), we want to solve the following min-max problem:

$$\min_{\theta} \frac{1}{N} \sum_{n=1}^N \max_{\delta \in \mathcal{U}} \mathcal{L}(y_n, \mathbf{z}^L(\theta, \mathbf{x}_n + \delta)), \quad (2)$$

for some uncertainty set  $\mathcal{U} \subset \mathbb{R}^M$ .  $\in \mathbb{R}^K$

Unfortunately, a closed form expression for the inner maximization problem above is unknown and solving the min-max problem is notoriously difficult. Robust optimization provides multiple tools for solving such problems when the loss function is either convex or concave in the input variables. For example, in the case of concave loss functions, a common approach would be to take the dual of the maximization problem so that the problem can be formulated as a single minimization problem (Bertsimas and den Hertog, 2022). If the loss function is instead convex, Fenchel's duality as well as conjugate functions can be used to find upper bounds and lower bounds of the maximization problem. However, there is no general framework developed for loss functions that do not fall into those categories, like in the case of neural networks. In this paper, we will focus on the specific case in which the uncertainty set is the ball of radius  $\rho$  in the  $L_p$  space; i.e.  $\mathcal{U} = \{\delta : \|\delta\|_p \leq \rho\}$ .

#### 4. Approximate Robust Upper Bound for small $\rho$

Perhaps the most intuitive approach to tackle problem (2) is to consider the first order approximation of the loss function

$$\mathcal{L}(y, \mathbf{z}^L(\theta, \mathbf{x} + \delta)) \approx \mathcal{L}(y, \mathbf{z}^L(\theta, \mathbf{x})) + \delta^\top \nabla_{\mathbf{x}} \mathcal{L}(y, \mathbf{z}^L(\theta, \mathbf{x})),$$

since the right hand side is a linear function of  $\delta$  and the maximization problem can be more easily solved for linear functions of the uncertainty. For example, it is not hard to see that the first order approximation reaches its maximum value in  $\mathcal{U} = \{\delta : \|\delta\|_\infty \leq \rho\}$  exactly at  $\delta^* = \rho \text{sign}(\nabla_{\mathbf{x}} \mathcal{L}(y, \mathbf{z}^L(\theta, \mathbf{x})))$ . This approach is referred to as *fast gradient sign method* and it was first explored in Goodfellow et al. (2015), where the networks are trained with adversarial examples

generated as  $\mathbf{x} + \boldsymbol{\delta}^*$ . A similar approach was proposed in Huang et al. (2016), where the authors considered the cross entropy loss and use the linear approximation of the softmax layer instead of the approximation of the entire loss function. In these examples, linear approximations are used to find near optimal perturbations that can produce strong adversarial examples for training, but not to modify the objective function.

An alternative to these methods would then be to train the network with the natural data and replace the loss function with its linear approximation, transforming the problem into

$$\begin{aligned} & \min_{\theta} \frac{1}{N} \sum_{n=1}^N \max_{\boldsymbol{\delta} \in \mathcal{U}} \mathcal{L}(y_n, \mathbf{z}^L(\theta, \mathbf{x}_n)) + \boldsymbol{\delta}^\top \nabla_{\mathbf{x}} \mathcal{L}(y_n, \mathbf{z}^L(\theta, \mathbf{x}_n)) \\ &= \min_{\theta} \frac{1}{N} \sum_{n=1}^N \mathcal{L}(y_n, \mathbf{z}^L(\theta, \mathbf{x}_n)) + \rho \|\nabla_{\mathbf{x}} \mathcal{L}(y_n, \mathbf{z}^L(\theta, \mathbf{x}_n))\|_q, \end{aligned} \quad (3)$$

where  $\|\cdot\|_q$  is the dual norm of  $\|\cdot\|_p$ , satisfying  $\frac{1}{p} + \frac{1}{q} = 1$ . However, this approach has not been very popular, since the loss function is highly nonlinear and the adversarial accuracy obtained by optimizing the linear approximation is much worse than the one obtained with adversarial training even for small values of  $\rho$  (see the Baseline method in Section 6). Nonetheless, from the network definitions in Section 3 we can see that each component of the network  $\mathbf{z}^L(\theta, \mathbf{x})$  is in fact a continuous piecewise linear function, suggesting that the first order approximation of  $\mathbf{z}^L$  is more precise than that of  $\mathcal{L}(y, \mathbf{z}^L)$ . In fact, we expect the outputs  $\mathbf{z}^L(\theta, \mathbf{x})$  and  $\mathbf{z}^L(\theta, \mathbf{x} + \boldsymbol{\delta})$  to be in the same linear piece when  $\mathbf{x} + \boldsymbol{\delta}$  is close to  $\mathbf{x}$ . In other words, the linear approximation

$$\mathbf{z}^L(\theta, \mathbf{x} + \boldsymbol{\delta}) \approx \mathbf{z}^L(\theta, \mathbf{x}) + \boldsymbol{\delta}^\top \nabla_{\mathbf{x}} \mathbf{z}^L(\theta, \mathbf{x}) \quad (4)$$

is exact for small enough  $\boldsymbol{\delta}$ . We can then approximately solve the adversarial problem for each class  $k$  as

$$\begin{aligned} \max_{\boldsymbol{\delta} \in \mathcal{U}} (\mathbf{e}_k - \mathbf{e}_y)^\top \mathbf{z}^L(\theta, \mathbf{x} + \boldsymbol{\delta}) &\approx \max_{\boldsymbol{\delta} \in \mathcal{U}} (\mathbf{e}_k - \mathbf{e}_y)^\top \mathbf{z}^L(\theta, \mathbf{x}) + \boldsymbol{\delta}^\top \nabla_{\mathbf{x}} (\mathbf{e}_k - \mathbf{e}_y)^\top \mathbf{z}^L(\theta, \mathbf{x}) \\ &= (\mathbf{e}_k - \mathbf{e}_y)^\top \mathbf{z}^L(\theta, \mathbf{x}) + \rho \|(\mathbf{e}_k - \mathbf{e}_y)^\top \nabla_{\mathbf{x}} \mathbf{z}^L(\theta, \mathbf{x})\|_q \\ &= \mathbf{c}_k^\top \mathbf{z}^L(\theta, \mathbf{x}) + \rho \|\mathbf{c}_k^\top \nabla_{\mathbf{x}} \mathbf{z}^L(\theta, \mathbf{x})\|_q, \end{aligned} \quad (5)$$

where  $\mathbf{e}_k$  refers to the one-hot vectors with a 1 in the  $k^{\text{th}}$  coordinate and 0 everywhere else, and  $\mathbf{c}_k$  is defined as  $\mathbf{c}_k := \mathbf{e}_k - \mathbf{e}_y$ . Since the loss functions utilized in deep learning for classification problems (cross-entropy loss, hinge loss, and zero-one loss) are monotone and transitionally invariant; i.e. they satisfy

$$\mathcal{L}(y, \mathbf{z}) = \mathcal{L}(y, \mathbf{z} - c\mathbf{1}) \quad \forall c \in \mathbb{R}, \quad (6)$$

we can use Eq. (5) to obtain an approximate upper bound of problem (2) as follows:

$$\min_{\theta} \max_{\boldsymbol{\delta} \in \mathcal{U}} \mathcal{L}(y, \mathbf{z}^L(\theta, \mathbf{x} + \boldsymbol{\delta})) \quad (7)$$

$$= \min_{\theta} \max_{\boldsymbol{\delta} \in \mathcal{U}} \mathcal{L}\left(y, \mathbf{z}^L(\theta, \mathbf{x} + \boldsymbol{\delta}) - \mathbf{e}_y^\top \mathbf{z}^L(\theta, \mathbf{x} + \boldsymbol{\delta}) \mathbf{1}\right), \quad (\text{By Eq. (6)}) \quad (8)$$

$$\leq \min_{\theta} \mathcal{L}\left(y, \left(\max_{\boldsymbol{\delta} \in \mathcal{U}} \mathbf{c}_1^\top \mathbf{z}^L(\theta, \mathbf{x} + \boldsymbol{\delta}), \dots, \max_{\boldsymbol{\delta} \in \mathcal{U}} \mathbf{c}_K^\top \mathbf{z}^L(\theta, \mathbf{x} + \boldsymbol{\delta})\right)\right), \quad (\text{By monotonicity}) \quad (9)$$

$$\approx \min_{\theta} \mathcal{L}\left(y, (\mathbf{c}_1^\top \mathbf{z}^L(\theta, \mathbf{x}) + \rho \|\mathbf{c}_1^\top \nabla_{\mathbf{x}} \mathbf{z}^L(\theta, \mathbf{x})\|_q, \dots, \mathbf{c}_K^\top \mathbf{z}^L(\theta, \mathbf{x}) + \rho \|\mathbf{c}_K^\top \nabla_{\mathbf{x}} \mathbf{z}^L(\theta, \mathbf{x})\|_q)\right). \quad (10)$$

(By Eq. (5))

Therefore, we propose to train the network by minimizing Eq. (10) instead of the standard average loss. For the particular case of the cross entropy loss with softmax activation function in the output layer, the exact optimization problem to be solved would be

$$\min_{\theta} \frac{1}{N} \sum_{n=1}^N \log \left( \sum_k e^{(\mathbf{e}_k - \mathbf{e}_{y_n})^\top \mathbf{z}^L(\theta; \mathbf{x}) + \rho \|\nabla_{\mathbf{x}}(\mathbf{e}_k - \mathbf{e}_{y_n})^\top \mathbf{z}^L(\theta; \mathbf{x})\|_q} \right). \quad (11)$$

Even though this expression is not guaranteed to be an upper bound of Eq. (2), we observe across a variety of experiments that Eq. (11) behaves like an upper bound of the adversarial loss (see Figure 1 and Table 1), indicating that the upper bound obtained by monotonicity in Eq. (9) generally counteracts the error from the first order approximation of  $\mathbf{z}^L$ .

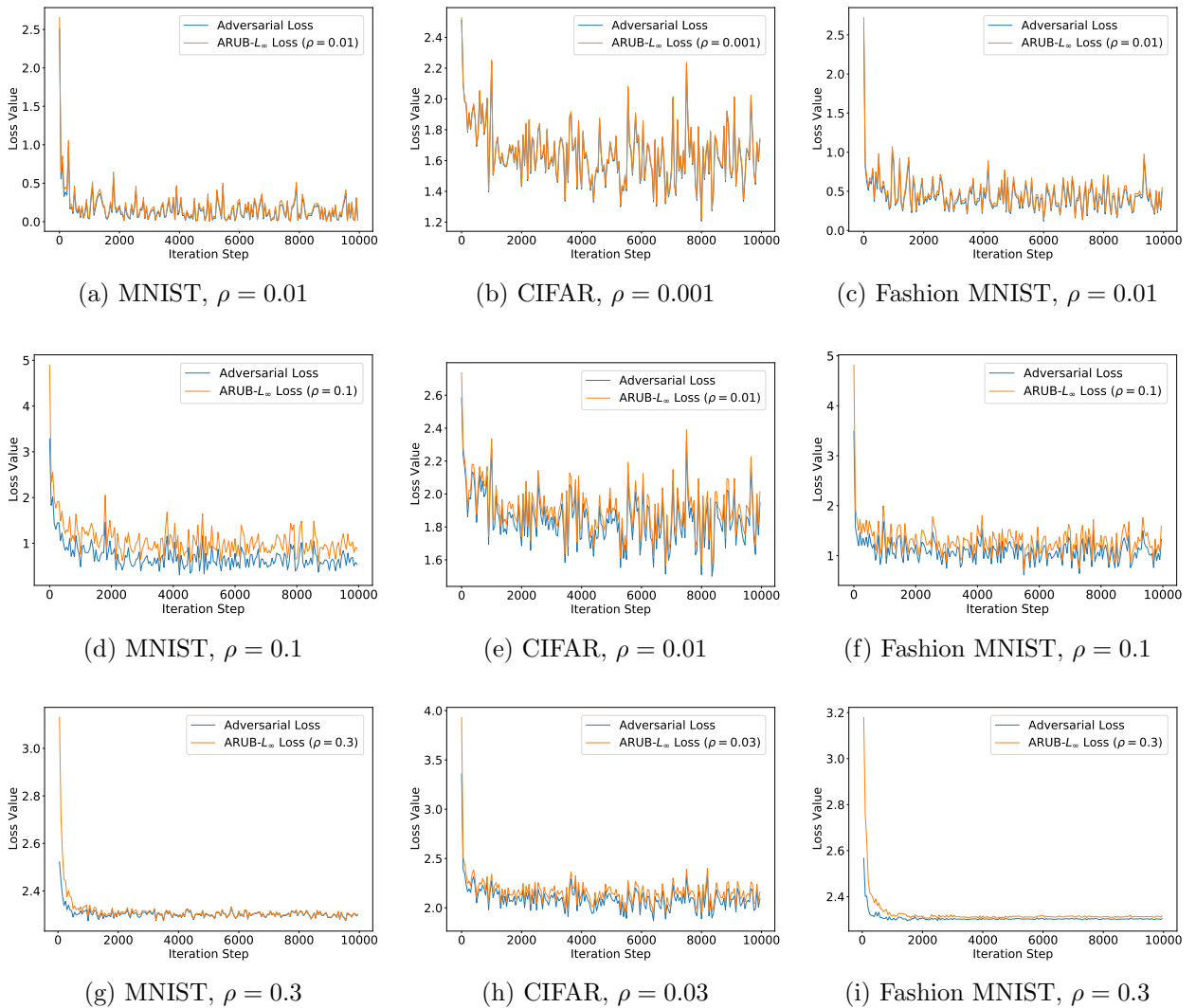


Figure 1: Adversarial loss (cross entropy loss evaluated at adversarial images bounded in  $L_\infty$  norm) vs the approximate upper bound (Eq. (11) evaluated at the natural images). The columns correspond to experiments with the MNIST, CIFAR, and Fashion MNIST data sets from left to right, and the value of  $\rho$  increases for lower rows.



	$\rho = 0.0$	0.0008	0.001	0.0015	0.002	0.003	0.01	0.1	0.3	0.5	1.0
$L_\infty$	0.94	0.99	0.99	0.99	0.99	0.99	0.99	0.95	0.86	0.81	0.79
$L_1$	0.933	0.99	0.99	0.99	0.99	0.99	0.99	0.99	0.99	0.99	0.98

Table 1: Percentage of times when the aRUB approach yields an upper bound of the adversarial cross entropy with respect to PGD attacks. For each row, both training methods use the  $L_p$  norm indicated on the first column. Percentages are computed across multiple networks trained with 46 UCI data sets.

## 5. Robust Upper bound for the $L_1$ norm and general $\rho$ .

In this section we derive an exact upper bound for the robust counterpart of the inner maximization problem in Eq. (2) for the specific case in which the uncertainty set is the ball of radius  $\rho$  in the  $L_1$  space; i.e.  $\mathcal{U} = \{\boldsymbol{\delta} : \|\boldsymbol{\delta}\|_1 \leq \rho\}$ . To find these upper bound we will use several tools from nonlinear and robust optimization. For this, we will make use of three lemmas that rely on the definition of conjugate functions as well as the Fenchel duality theorem, and their proofs can be found in Appendix A. Together, these lemmas are the core of the methodology presented in this section.

In the robust optimization framework, finding a safe approximation (or the exact robust counterpart) for a problem that is convex (or concave) in the uncertainty parameters relies on using convex (or concave) conjugate functions to make the problem linear in the uncertainty (Bertsimas and den Hertog, 2022). The following lemmas are a generalization of this approach for the case in which the objective involves the composition of two functions, with the goal of making the problem linear not in the uncertainty but in the inner most function. Lemma 1 makes this generalization when the outer function is convex while Lemma 2 focuses on the concave case.

**Lemma 1** *If  $f : A \rightarrow B$  is a convex and closed function then for any function  $\mathbf{z} : \mathcal{U} \rightarrow A$ , and any function  $g : A \rightarrow B$  we have*

$$\sup_{\boldsymbol{\delta} \in \mathcal{U}} f(\mathbf{z}(\boldsymbol{\delta})) + g(\mathbf{z}(\boldsymbol{\delta})) = \sup_{\mathbf{u} \in \text{dom}(f^*)} \sup_{\boldsymbol{\delta} \in \mathcal{U}} \mathbf{z}(\boldsymbol{\delta})^T \mathbf{u} - f^*(\mathbf{u}) + g(\mathbf{z}(\boldsymbol{\delta})),$$

where the convex conjugate function  $f^*$  is defined by  $f^*(\mathbf{z}) = \sup_{\mathbf{x} \in \text{dom}(f)} \mathbf{z}^T \mathbf{x} - f(\mathbf{x})$ .

**Proof** See Appendix A1. ■

**Lemma 2** *Let  $g : A \rightarrow B$  be a concave and closed function. If a function  $\mathbf{z} : \mathcal{U} \rightarrow A$  satisfies  $g(\mathbf{z}(\boldsymbol{\delta})) < \infty$  for all  $\boldsymbol{\delta} \in \mathcal{U}$ , then*

$$\sup_{\boldsymbol{\delta} \in \mathcal{U}} g(\mathbf{z}(\boldsymbol{\delta})) = \inf_{\mathbf{v} \in \text{dom}(g_*)} \sup_{\boldsymbol{\delta} \in \mathcal{U}} \mathbf{z}(\boldsymbol{\delta})^T \mathbf{v} - g_*(\mathbf{v}),$$

where the concave conjugate function is defined by  $g_*(\mathbf{z}) = \inf_{\mathbf{x} \in \text{dom}(g)} \mathbf{z}^T \mathbf{x} - g(\mathbf{x})$ .

**Proof** See Appendix A2. ■

From the lemmas above we can observe that to apply them we will need to compute convex and concave conjugate functions. The next lemma facilitates this computations for neural networks with ReLU activation functions.

**Lemma 3** *If  $\mathbf{u}, \mathbf{p}, \mathbf{q} \geq \mathbf{0}$ , then the functions  $f(\mathbf{x}) = \mathbf{p}^\top [\mathbf{x}]^+$  and  $g(\mathbf{x}) = \mathbf{x}^\top \mathbf{u} - \mathbf{q}^\top [\mathbf{x}]^+$  satisfy*

$$a) f^*(\mathbf{z}) = \begin{cases} 0 & \text{if } \mathbf{0} \leq \mathbf{z} \leq \mathbf{p}, \\ \infty & \text{otherwise.} \end{cases} \quad \text{and} \quad b) g_*(\mathbf{z}) = \begin{cases} 0 & \text{if } \mathbf{u} - \mathbf{q} \leq \mathbf{z} \leq \mathbf{u}, \\ -\infty & \text{otherwise.} \end{cases}$$

**Proof** See Appendix A3. ■

As observed in Eqs. (7) to (9), we can obtain an upper bound of the min-max problem in Eq. (2) by finding instead upper bounds for  $\max_{\delta \in \mathcal{U}} (\mathbf{e}_k - \mathbf{e}_y)^\top \mathbf{z}^L(\theta, \mathbf{x} + \delta)$  for each class  $k$ . We will find these upper bounds by recursively applying the previous lemmas in each layer of the network. Starting from the last layer, at each stage we split the model as the sum of a convex function and a concave function, and we then apply Lemmas 1 and 2 to move the supremum over  $\mathcal{U}$  towards the previous layer until we reach the first layer of the network. Since this first layer is linear in the uncertainty and the dual function of the  $L_1$  norm is the  $L_\infty$  norm (a maximum over a finite set), we are able to exactly solve the maximization problem over  $\mathcal{U}$  and to backtrack to solve for the variables  $\mathbf{u}, \mathbf{v}$  that lemmas 1 and 2 introduce.

For simplicity, we develop and prove the upper bound for the robust counterpart assuming that the neural network has only two layers; however the results can be extended to the general case as shown in Appendix B. In addition, all the theorems can be generalized for convolutions neural networks, since convolutions are a special case of matrix multiplication.

The following theorem, whose proof relies on Lemmas 1 and 2, shows how the supremum over  $\mathcal{U}$  can be moved from the second layer to the first layer.

**Theorem 4** *The maximum difference between the output of the correct class and the output of any other class  $k$  can be written as*

$$\begin{aligned} & \sup_{\delta \in \mathcal{U}} \mathbf{c}_k^\top \mathbf{z}^2(\theta, \mathbf{x} + \delta) & (12) \\ = & \sup_{0 \leq \mathbf{s} \leq \mathbf{1}} \inf_{0 \leq \mathbf{t} \leq \mathbf{1}} \sup_{\delta \in \mathcal{U}} (\mathbf{p} - \mathbf{q})^\top \mathbf{z}^1(\theta, \mathbf{x} + \delta) + \mathbf{c}_k^\top \mathbf{b}^2 \\ & \text{s.t. } \mathbf{p} = [(\mathbf{W}^2)^\top \mathbf{c}_k]^+ \odot \mathbf{s} & (13) \\ & \mathbf{q} = [-(\mathbf{W}^2)^\top \mathbf{c}_k]^+ \odot \mathbf{t}, \end{aligned}$$

where  $\odot$  corresponds to entry-wise multiplication.

**Proof** By definition of the two layer neural network  $\mathbf{z}^2$ , we have

$$\begin{aligned}\mathbf{c}_k^\top \mathbf{z}^2(\theta, \mathbf{x} + \boldsymbol{\delta}) &= \mathbf{c}_k^\top \mathbf{W}^2 [\mathbf{z}^1(\theta, \mathbf{x} + \boldsymbol{\delta})]^+ + \mathbf{c}_k^\top \mathbf{b}^2 \\ &= f_+(\mathbf{z}^1(\theta, \mathbf{x} + \boldsymbol{\delta})) - f_-(\mathbf{z}^1(\theta, \mathbf{x} + \boldsymbol{\delta})) + \mathbf{c}_k^\top \mathbf{b}^2,\end{aligned}$$

where  $f_+, f_-$  are the convex functions defined by

$$f_+(\mathbf{x}) = [\mathbf{c}_k^\top \mathbf{W}^2]^+ [\mathbf{x}]^+, \quad \text{and} \quad f_-(\mathbf{x}) = [-\mathbf{c}_k^\top \mathbf{W}^2]^+ [\mathbf{x}]^+.$$

Applying Lemma 1 to the function  $f_+$  we then have

$$\begin{aligned}& \sup_{\boldsymbol{\delta} \in \mathcal{U}} \mathbf{c}_k^\top \mathbf{z}^2(\theta, \mathbf{x} + \boldsymbol{\delta}), \\ &= \sup_{\boldsymbol{\delta} \in \mathcal{U}} f_+(\mathbf{z}^1(\theta, \mathbf{x} + \boldsymbol{\delta})) - f_-(\mathbf{z}^1(\theta, \mathbf{x} + \boldsymbol{\delta})) + \mathbf{c}_k^\top \mathbf{b}^2, \\ &= \sup_{\mathbf{u} \in \text{dom}(f_+^*)} \sup_{\boldsymbol{\delta} \in \mathcal{U}} \mathbf{u}^\top \mathbf{z}^1(\theta, \mathbf{x} + \boldsymbol{\delta}) - f_+^*(\mathbf{u}) - f_-(\mathbf{z}^1(\theta, \mathbf{x} + \boldsymbol{\delta})) + \mathbf{c}_k^\top \mathbf{b}^2, \quad (\text{By Lemma 1}), \quad (14)\end{aligned}$$

$$= \sup_{\mathbf{u} \in \text{dom}(f_+^*)} \sup_{\boldsymbol{\delta} \in \mathcal{U}} \mathbf{u}^\top \mathbf{z}^1(\theta, \mathbf{x} + \boldsymbol{\delta}) - f_-(\mathbf{z}^1(\theta, \mathbf{x} + \boldsymbol{\delta})) + \mathbf{c}_k^\top \mathbf{b}^2, \quad (\text{By Lemma 3a}). \quad (15)$$

Defining the concave function  $g(\mathbf{x}) = \mathbf{u}^\top \mathbf{x} - f_-(\mathbf{x})$ , and applying Lemma 2 to the function  $g$  we obtain

$$\begin{aligned}& \sup_{\boldsymbol{\delta} \in \mathcal{U}} \mathbf{c}_k^\top \mathbf{z}^2(\theta, \mathbf{x} + \boldsymbol{\delta}) \\ &= \sup_{\mathbf{u} \in \text{dom}(f_+^*)} \sup_{\boldsymbol{\delta} \in \mathcal{U}} g(\mathbf{z}^1(\theta, \mathbf{x} + \boldsymbol{\delta})) + \mathbf{c}_k^\top \mathbf{b}^2 \quad (16)\end{aligned}$$

$$= \sup_{\mathbf{u} \in \text{dom}(f_+^*)} \inf_{\mathbf{v} \in \text{dom}(g_*)} \sup_{\boldsymbol{\delta} \in \mathcal{U}} \mathbf{v}^\top \mathbf{z}^1(\theta, \mathbf{x} + \boldsymbol{\delta}) - g_*(\mathbf{v}) + \mathbf{c}_k^\top \mathbf{b}^2 \quad (\text{By Lemma 2}), \quad (17)$$

$$= \sup_{\mathbf{u} \in \text{dom}(f_+^*)} \inf_{\mathbf{v} \in \text{dom}(g_*)} \sup_{\boldsymbol{\delta} \in \mathcal{U}} \mathbf{v}^\top \mathbf{z}^1(\theta, \mathbf{x} + \boldsymbol{\delta}) + \mathbf{c}_k^\top \mathbf{b}^2 \quad (\text{By Lemma 3b}). \quad (18)$$

Lastly, by Lemma 3a and 3b, we know that the variables  $\mathbf{u}$  and  $\mathbf{v}$  can be parameterized as

$$\begin{aligned}\mathbf{u} &= [(\mathbf{W}^2)^\top \mathbf{c}_k]^+ \odot \mathbf{s}, \\ \mathbf{v} &= [(\mathbf{W}^2)^\top \mathbf{c}_k]^+ \odot \mathbf{s} - [-(\mathbf{W}^2)^\top \mathbf{c}_k]^+ \odot \mathbf{t}\end{aligned}$$

with  $0 \leq \mathbf{s}, \mathbf{t} \leq 1$ . Substituting these values in Eq. (18) we obtain Eq. (13), as desired.  $\blacksquare$

Notice that the objective in Eq. (13) is linear in  $\mathbf{z}^1$  and therefore it is also linear in  $\boldsymbol{\delta}$ , which facilitates the computation of the exact value of the supremum over  $\mathcal{U}$ , as shown in the next corollary.

**Corollary 5** *If  $\mathcal{U} = \{\boldsymbol{\delta} : \|\boldsymbol{\delta}\|_p \leq \rho\}$ , then:*

$$\sup_{\boldsymbol{\delta} \in \mathcal{U}} \mathbf{c}_k^\top \mathbf{z}^2(\theta, \mathbf{x} + \boldsymbol{\delta}) \quad (19)$$

$$= \sup_{0 \leq \mathbf{s} \leq 1} \inf_{0 \leq \mathbf{t} \leq 1} \rho \|(\mathbf{p} - \mathbf{q})^\top \mathbf{W}^1\|_q + (\mathbf{p} - \mathbf{q})^\top (\mathbf{W}^1 \mathbf{x} + \mathbf{b}^1) + \mathbf{c}_k^\top \mathbf{b}^2$$

$$\begin{aligned}s.t. \quad \mathbf{p} &= [(\mathbf{W}^2)^\top \mathbf{c}_k]^+ \odot \mathbf{s} \\ \mathbf{q} &= [-(\mathbf{W}^2)^\top \mathbf{c}_k]^+ \odot \mathbf{t},\end{aligned} \quad (20)$$

where  $\|\cdot\|_q$  is the dual norm of  $\|\cdot\|_p$ , with  $\frac{1}{p} + \frac{1}{q} = 1$ .

Before proceeding to the proof of the corollary, notice that we can recover the approximation method developed in the previous section by setting

$$\mathbf{s} = \mathbf{t} = [\text{sign}(\mathbf{z}^1(\theta, \mathbf{x}))]^+ \quad (21)$$

in the objective of problem (20) to obtain

$$\rho \|((\mathbf{W}^2)^\top \mathbf{c}_k \odot [\text{sign}(\mathbf{z}^1(\theta, \mathbf{x}))]^+)^\top \mathbf{W}^1\|_q + \mathbf{c}_k^\top \mathbf{W}^2 [\mathbf{z}^1(\theta, \mathbf{x})]^+ + \mathbf{c}_k^\top \mathbf{b}^2, \quad (22)$$

which is the same as the linear approximation of  $\mathbf{c}_k^\top \mathbf{z}^2(\theta + \boldsymbol{\delta})$  obtained in Eq. (5).

**Proof** The proof follows directly after applying Theorem 4 and using the fact that for all vectors  $\mathbf{c}$  we have

$$\sup_{\boldsymbol{\delta}: \|\boldsymbol{\delta}\|_p \leq \rho} \mathbf{c}^\top \boldsymbol{\delta} = \rho \|\mathbf{c}\|_q. \quad (23)$$

■

Since neural networks are trained by minimizing the empirical loss over the parameters  $\theta$ , we want to avoid the computation of supremums in the objective. While the previous corollary shows how to solve the supremum over the uncertainty set, a new supremum was introduced in Theorem 4 over the variables  $\mathbf{s}$ . The next theorem tells us how we can remove this new supremums for the specific case  $p = 1$ .

**Theorem 6** *The maximum difference between the output of the correct class and the output of any other class  $k$  can be upper bounded by*

$$\begin{aligned} & \sup_{\boldsymbol{\delta}: \|\boldsymbol{\delta}\|_1 \leq \rho} \mathbf{c}_k^\top \mathbf{z}^2(\theta, \mathbf{x} + \boldsymbol{\delta}) \\ & \leq \inf_{0 \leq t \leq 1} \max_{m \in [M]} \max \left\{ g_{k,m}^2(\theta, \mathbf{t}, \mathbf{x}, \rho), g_{k,m}^2(\theta, \mathbf{t}, \mathbf{x}, -\rho) \right\}, \end{aligned} \quad (24)$$

where the new network  $g$  is defined by the equations

$$\begin{aligned} g_m^1(\theta, a) &= a \mathbf{W}^1 \mathbf{e}_m + \mathbf{W}^1 \mathbf{x} + \mathbf{b}^1, \\ g_{k,m}^2(\theta, \mathbf{t}, \mathbf{x}, a) &= [\mathbf{c}_k^\top \mathbf{W}^2]^+ [g_m^1(\theta, a)]^+ - [-\mathbf{c}_k^\top \mathbf{W}^2]^+ [g_m^1(\theta, a)] \odot \mathbf{t} + \mathbf{c}_k^\top \mathbf{b}^2, \end{aligned}$$

for  $a = \rho, -\rho$ .

**Proof** Applying Corollary 5 with  $p = 1$  and using the min-max inequality we obtain

$$\sup_{\boldsymbol{\delta}: \|\boldsymbol{\delta}\|_1 \leq \rho} \mathbf{c}_k^\top \mathbf{z}^2(\theta, \mathbf{x} + \boldsymbol{\delta}) \quad (25)$$

$$\begin{aligned} & \leq \inf_{0 \leq t \leq 1} \sup_{0 \leq s \leq 1} \rho \|(\mathbf{p} - \mathbf{q})^\top \mathbf{W}^1\|_\infty + (\mathbf{p} - \mathbf{q})^\top (\mathbf{W}^1 \mathbf{x} + \mathbf{b}^1) + \mathbf{c}_k^\top \mathbf{b}^2 \\ & \quad \text{s.t. } \mathbf{p} = [(\mathbf{W}^2)^\top \mathbf{c}_k]^+ \odot \mathbf{s} \\ & \quad \mathbf{q} = [-(\mathbf{W}^2)^\top \mathbf{c}_k]^+ \odot \mathbf{t}. \end{aligned} \quad (26)$$

Defining  $\mathbf{p}(\mathbf{s}) = [(\mathbf{W}^2)^\top \mathbf{c}_k]^+ \odot \mathbf{s}$  and  $\mathbf{q}(\mathbf{t}) = [-(\mathbf{W}^2)^\top \mathbf{c}_k]^+ \odot \mathbf{t}$ , we have that for fixed  $\mathbf{t}$  it holds

$$\begin{aligned}
& \sup_{0 \leq \mathbf{s} \leq 1} \rho \|(\mathbf{p}(\mathbf{s}) - \mathbf{q}(\mathbf{t}))^\top \mathbf{W}^1\|_\infty + (\mathbf{p}(\mathbf{s}) - \mathbf{q}(\mathbf{t}))^\top (\mathbf{W}^1 \mathbf{x} + \mathbf{b}^1) + \mathbf{c}_k^\top \mathbf{b}^2 \\
&= \max_{m \in [M]} \max \left\{ \sup_{0 \leq \mathbf{s} \leq 1} (\mathbf{p}(\mathbf{s}) - \mathbf{q}(\mathbf{t}))^\top (\mathbf{W}^1 (\mathbf{x} + \rho \mathbf{e}_m) + \mathbf{b}^1) + \mathbf{c}_k^\top \mathbf{b}^2, \right. \\
&\quad \left. \sup_{0 \leq \mathbf{s} \leq 1} (\mathbf{p}(\mathbf{s}) - \mathbf{q}(\mathbf{t}))^\top (\mathbf{W}^1 (\mathbf{x} - \rho \mathbf{e}_m) + \mathbf{b}^1) + \mathbf{c}_k^\top \mathbf{b}^2 \right\} \\
&= \max_{m \in [M]} \max \left\{ [\mathbf{c}_k^\top \mathbf{W}^2]^+ [\mathbf{W}^1 (\mathbf{x} + \rho \mathbf{e}_m) + \mathbf{b}^1]^+ - \mathbf{q}(\mathbf{t})^\top (\mathbf{W}^1 (\mathbf{x} + \rho \mathbf{e}_m) + \mathbf{b}^1) + \mathbf{c}_k^\top \mathbf{b}^2, \right. \\
&\quad \left. [(\mathbf{c}_k^\top \mathbf{W}^2)^+ [\mathbf{W}^1 (\mathbf{x} - \rho \mathbf{e}_m) + \mathbf{b}^1]^+ - \mathbf{q}(\mathbf{t})^\top (\mathbf{W}^1 (\mathbf{x} - \rho \mathbf{e}_m) + \mathbf{b}^1) + \mathbf{c}_k^\top \mathbf{b}^2] \right\} \\
&= \max_{m \in [M]} \max \{g_{k,m}^2(\theta, \mathbf{t}, \mathbf{x}, \rho), g_{k,m}^2(\theta, \mathbf{t}, \mathbf{x}, -\rho)\}.
\end{aligned}$$

The theorem then follows after applying the inf over  $0 \leq \mathbf{t} \leq 1$ . ■

Notice that in the previous proof it was crucial to use  $p = 1$ , since the dual of the  $L_1$  norm is the  $L_\infty$  norm, which can be written as a maximum over a finite set. With a different  $p$  we would not have been able to apply the same technique to remove the variables  $\mathbf{s}$ . However, for the chosen uncertainty set we obtain an upper bound of Eq. (2) by applying the result from the previous Theorem to Eq. (9).

While we could include the variables  $\mathbf{t}$  in the minimization problem over  $\theta$ , we instead use fixed values  $\mathbf{t} = [\text{sign}(\mathbf{z}^1(\theta, \mathbf{x}))]^+$  based on the linear approximation of  $\mathbf{c}_k^\top \mathbf{z}^2(\theta, \mathbf{x} + \boldsymbol{\delta})$ , as described in Eq. (21). Notice that setting specific values for  $\mathbf{t}$  does not affect the inequalities: since the upper bound includes the infimum over  $\mathbf{t}$ , any  $0 \leq \mathbf{t} \leq 1$  yields an upper bound of the robust problem. For the specific case of the cross entropy loss function, the proposed upper bound for the min-max robust problem is

$$\min_{\theta} \frac{1}{N} \sum_{n=1}^N \log \left( \sum_k e^{\left( \max_{m \in [M]} \max \{g_{k,m}^2(\theta, [\text{sign}(\mathbf{z}^1(\theta, \mathbf{x}))]^+, \mathbf{x}, \rho), g_{k,m}^2(\theta, [\text{sign}(\mathbf{z}^1(\theta, \mathbf{x}))]^+, \mathbf{x}, -\rho)\} \right)} \right). \quad (27)$$

## 6. Experiments

In this section, we demonstrate the effectiveness of the proposed methods in practice. We first introduce the experimental setup and then we compare the robustness of several defenses.

### 6.1 Experimental details

**Data sets.** We use 46 data sets from the UCI collection (Dua and Graff, 2017), which correspond to classification tasks with a diverse number of features that are not categorical. For each data set we do a 80%/20% split for training/testing sets, and we further reserve 25% of each training set for

validation. In addition, we use three popular computer vision data sets, namely the MNIST (Deng, 2012), Fashion MNIST (Xiao et al., 2017) and CIFAR (Krizhevsky, 2009) data sets.

**Pre-processing.** All input data has been previously scaled, which facilitates the comparison of the adversarial attacks across data sets. For the UCI data sets, each feature is standardized using the statistics of the training set, while for the vision data sets each image channel is normalized to be between 0 and 1, or standardized, depending on what leads to best robustness.

**Attacks.** We use the implementation provided by the foolbox library (Rauber et al., 2017,0) using the default parameters. We evaluate the PGD, FGM and FGSM attacks. More specifically, we use the following attacks:

- PGD- $L_p$ : Adversarial attack bounded in  $L_p$  norm and found using Projected Gradient Descent.
- FGM- $L_p$ : Adversarial attack bounded in  $L_p$  norm and found using Fast Gradient Method.
- FSGM- $L_p$ : Adversarial attack bounded in  $L_p$  norm and found using Fast Sign Gradient Method.

For the UCI data sets we evaluate adversarial accuracies with respect to attacks bounded in  $L_1$ ,  $L_2$  and  $L_\infty$  norm. For the vision data sets, we present results only for attacks bounded in the  $L_2$  norm, but results using other attacks can be found in Appendix C.

**Defenses.** Our comparisons include different defenses denoted as follows:

- ARUB- $L_p$ : Approximate Robust Upper Bound method described in section 4 using the  $L_1$  or  $L_\infty$  sphere as the uncertainty set.
- RUB: Robust Upper Bound method described in section 5 using the  $L_1$  sphere as the uncertainty set.
- PGD- $L_\infty$ : Adversarial training method in which the attacks are bounded in the  $L_\infty$  norm and found using Projected Gradient Descent.
- Nominal: Standard vanilla training with no robustness ( $\rho = 0$ ).
- Baseline- $L_\infty$ : Simple approximation method resulting from minimizing Eq. (3) using the  $L_p$  sphere as the uncertainty set.

**Architecture.** We evaluate a neural network with three dense hidden layers with 200 neurons in each hidden layer. For the vision datasets, we also provide results with Convolutional Neural Networks (*CNNs*) in Appendix D. The architecture has two convolutional layers alternated with pooling operations, and two dense layers, as in Madry et al. (2019).

**Hyperparameter Tuning.** Each network and defense is trained multiple times for different learning rates ( $\{1, 10^{-1}, 10^{-2}, 10^{-3}, 10^{-4}, 10^{-5}, 10^{-6}\}$ ). For the UCI data set we use a batch size of 256 and for the vision data sets we try a batch size of 32 and 256. All networks trained using the UCI data sets are trained for 5000 iterations, and all vision data sets are trained for 10000 iteration which is sufficient for convergence in both cases. For the  $L_\infty$  based training methods we try all values of  $\rho$  from the set ( $\{10^{-4}, 10^{-5}, 10^{-3}, 10^{-2}, 0.1, 0.3, 0.5, 1, 3, 5, 10\}$ ). For the methods based on the  $L_1$  norm, we scale those values of  $\rho$  by a factor of  $\sqrt{m}$ , since  $\|\mathbf{x}\|_\infty \leq \|\mathbf{x}\|_2$  and  $\|\mathbf{x}\|_1 \leq \sqrt{m}\|\mathbf{x}\|_2$  for any  $\mathbf{x} \in \mathbb{R}^m$ . In this way we ensure that the  $L_1$  spheres and the  $L_\infty$  spheres contain the same  $L_2$  spheres, allowing for a fair comparison of all methods in terms of adversarial attacks that are bounded in the  $L_2$  norm. For each attack and each  $\rho$  of the attack, we select on the validation set the best hyperparameters for each defense.

## 6.2 UCI data sets

We run experiments on the 46 UCI data sets using different methods for robust training and compare the adversarial accuracies achieved with multiple types of adversarial attacks. For each data set we rank every training method, where the method with rank 1 corresponds to the one with highest adversarial accuracy. The results are shown in Figure 2, where we observe a similar pattern across all types of attacks, namely, we see that the best ranks are achieved with ARUB- $L_\infty$  and PGD- $L_\infty$  when  $\rho$  is smaller than  $10^{-1}$ ; next there is a small range in which PGD- $L_\infty$  does best and finally for larger values of  $\rho$  the best rank is that of RUB. We also highlight that looking at  $\rho = 0$ , it is clear that robust training methods achieve better natural accuracy than the one obtained with Nominal training.

To better compare the performances of RUB and PGD- $L_\infty$ , in Figure 3 we show the number of data sets for which RUB improves  $L_2$  adversarial accuracy over PGD- $L_\infty$  by a specific percentage. We observe that the improvement becomes more significant as  $\rho$  increases, and in particular, for  $\rho = 10$  we observe that RUB only lowers adversarial accuracy for 3 data sets, while it shows more than 15% improvement over PGD- $L_\infty$  for 8 of the data sets.

Lastly, in Table 2 we display the total training time of each method in a log scale. As expected, we see that nominal is the fastest training method, and while ARUB- $L_\infty$  and RUB increase the total time by several orders of magnitude, they are significantly faster than PGD- $L_\infty$ .

	Avg no. samples per second	Standard Deviation
RUB	9.71	8.07
ARUB - $L_\infty$	8.47	4.74
Baseline- $L_\infty$	11.69	9.58
PGD - $L_\infty$	7.06	2.60
Nominal	12.11	10.02

Table 2: Average log of the number of samples processed per second across the 46 UCI data sets, as well as the corresponding log of the standard deviations.

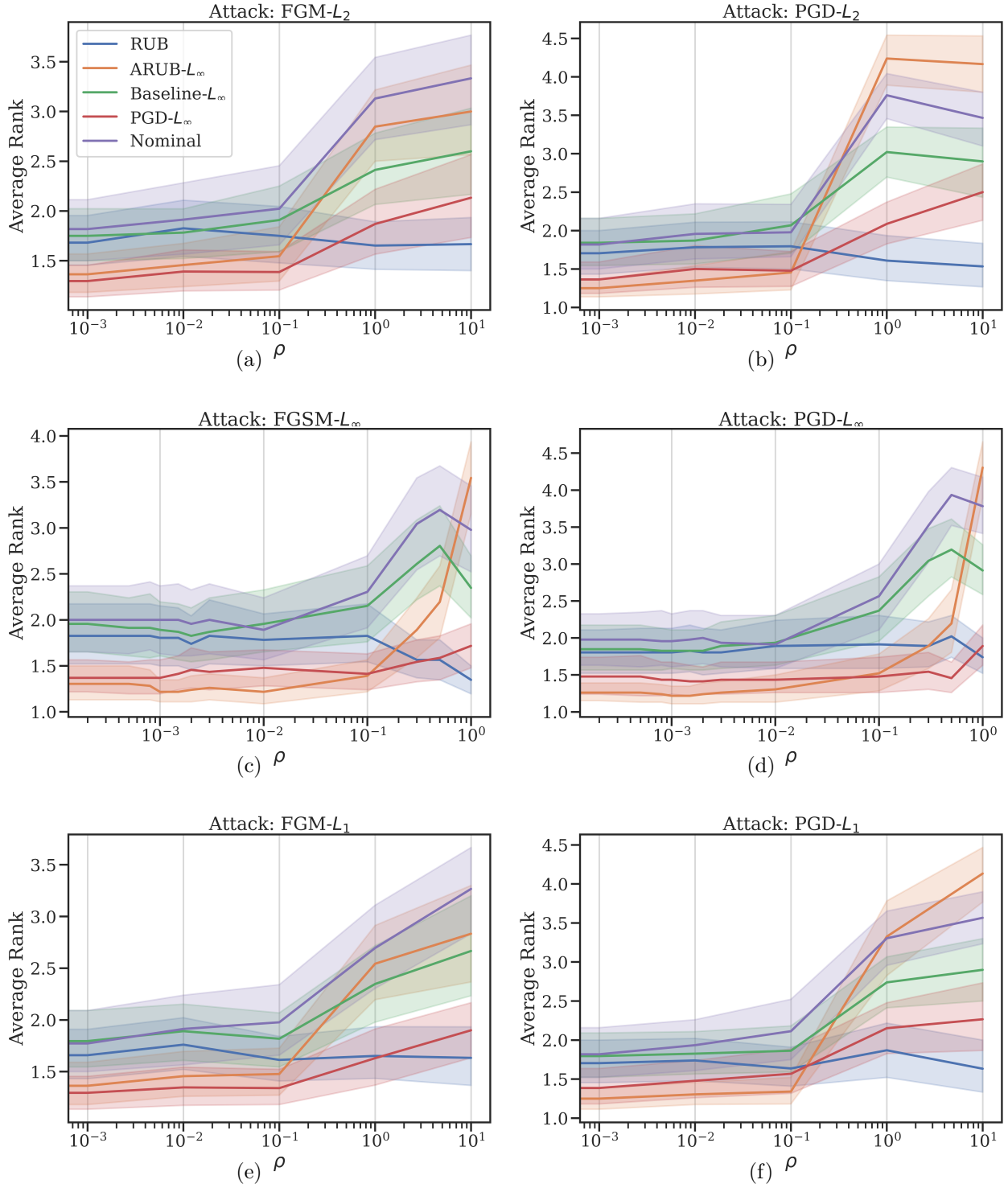


Figure 2: Average rank of each method across the 46 UCI data sets for adversarial attacks bounded in  $L_2$ ,  $L_\infty$  and  $L_1$  norm, respectively from top to bottom. The figures on the left use attacks based on Fast Gradient methods, and the figures on the right use instead attacks based on Projected Gradient Descent.



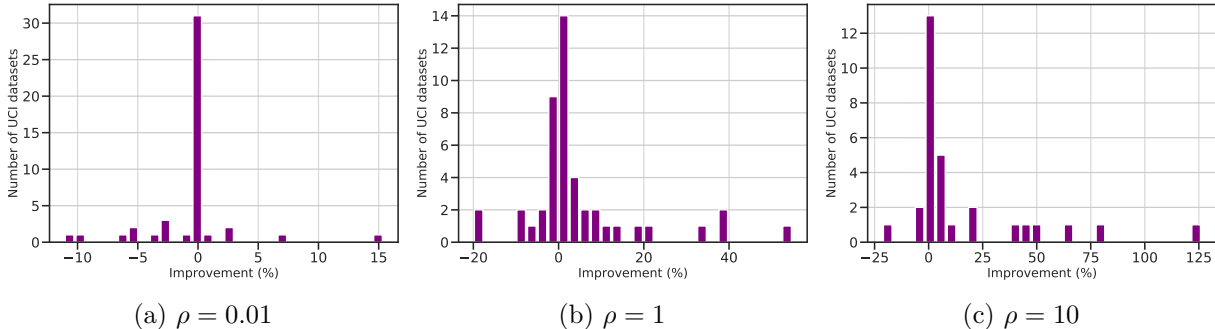


Figure 3: Number of UCI data sets for which RUB- $L_1$  improves adversarial accuracy over PGD- $L_\infty$  by a specific percentage. Figures a), b) and c) show the corresponding plots for PGD- $L_2$  adversarial examples with different values of  $\rho$ .

### 6.3 Vision Data Sets

We next show experiment results for the three vision data sets. Specifically, we compare for different training methods their performance against adversarial attacks as well as the security guarantees obtained from applying the upper bound from Eq. (27). We report adversarial accuracies using PGD- $L_2$  attacks. Also, adversarial accuracies using attacks bounded in  $L_1$  and  $L_\infty$  norms can be found in Appendix C. Moreover, since the proposed RUB method significantly increases memory requirements for inputs with large dimensions, we compare this method against other defenses using only the feed architecture with three hidden layers. We do include results using a CNN architecture for all other methods in Appendix D, where we also explain how to extend the theory of the RUB method for convolutional layers with ReLU and MaxPool activation functions.

**Performance Against Adversarial Attacks.** We evaluate adversarial accuracy for 6 different methods: RUB, ARUB- $L_1$ , ARUB- $L_\infty$ , Baseline- $L_\infty$ , PGD- $L_\infty$ , and Nominal training. We observe that for the Fashion MNIST data set (Table 3) as well as the MNIST data set (Table 4), ARUB- $L_1$  achieves the best accuracies for small values of  $\rho$ ; we then observe a small range in which PGD- $L_\infty$  does best and lastly for larger values of  $\rho$  we see that RUB takes the lead, which is similar to the average results observed for the UCI data sets. For the CIFAR data set we observe a different behavior; PGD- $L_\infty$  achieves better accuracies for small and large values of  $\rho$ , although we observe that all methods perform very poorly overall as this is a notoriously more difficult data set. Lastly, once again we observe that in all three data sets the robust training methods achieve a higher natural accuracy than the accuracy resulting from standard nominal training.

**Security Guarantees against  $L_1$  Norm Bounded Attacks.** Finally, we use the upper bound of the robust loss derived in section 4 to find lower bounds for the adversarial accuracy with respect to attacks bounded in the  $L_1$  norm by  $\rho$ . In Figures 8, 6 and 7 we observe that, as expected, for all three data sets, CIFAR, Fashion MNIST and MNIST, the best security guarantees are the ones for the RUB method. While these results are only lower bounds for the adversarial accuracy and we cannot claim a better accuracy for RUB than for the rest of the methods, the lower bound for the RUB method shows that this method indeed performs very well against  $L_1$  attacks bounded by large values of  $\rho$ . For instance, in Table 6 we can see that for the Fashion MNIST data set the RUB method guarantees 86.02% adversarial accuracy (less than 5% decrease from the best

$\rho =$	0.00	0.01	0.06	0.28	2.80	8.40	14.00	28.00
RUB	90.59	89.88	88.95	<b>86.80</b>	63.09	<b>56.95</b>	<b>57.07</b>	<b>55.27</b>
ARUB- $L_1$	<b>90.31</b>	<b>90.04</b>	<b>89.45</b>	85.98	66.17	30.63	18.24	15.04
ARUB- $L_\infty$	89.18	89.06	88.75	85.98	67.11	24.18	18.24	16.02
Baseline- $L_\infty$	89.38	89.02	88.32	85.39	50.20	29.88	28.71	26.52
PGD- $L_\infty$	89.61	89.38	88.01	85.23	<b>68.20</b>	31.60	25.90	22.85
Nominal	87.70	88.44	88.01	85.35	46.60	19.92	16.84	15.39

Table 3: Adversarial Accuracy for Fashion MNIST with PGD- $L_2$  attacks

$\rho =$	0.00	0.01	0.06	0.28	2.80	8.40	14.00	28.00
RUB	97.93	97.89	97.07	97.50	79.80	<b>66.48</b>	<b>62.89</b>	<b>55.00</b>
ARUB- $L_1$	<b>98.63</b>	<b>98.52</b>	97.73	97.46	81.13	57.58	55.04	46.60
ARUB- $L_\infty$	97.97	98.09	97.81	<b>98.28</b>	92.62	51.80	49.88	43.40
Baseline- $L_\infty$	97.58	97.50	97.58	97.11	72.85	64.18	61.29	52.81
PGD- $L_\infty$	98.24	98.32	<b>98.24</b>	98.09	<b>93.12</b>	66.05	62.46	54.26
Nominal	97.62	97.46	97.34	96.52	69.80	19.57	18.63	17.70

Table 4: Adversarial Accuracy for MNIST with PGD- $L_2$  attacks

$\rho =$	0.00	0.01	0.06	0.55	5.54	16.63	27.71	55.43
RUB	51.17	50.23	48.59	44.14	20.62	9.96	9.96	9.96
ARUB- $L_1$	52.70	51.41	<b>51.13</b>	<b>46.99</b>	<b>23.79</b>	9.69	9.30	9.30
ARUB- $L_\infty$	53.83	52.89	47.77	41.37	22.66	11.48	11.52	11.56
Baseline- $L_\infty$	53.12	52.07	46.52	37.19	9.30	9.30	9.30	9.30
PGD- $L_\infty$	<b>53.91</b>	<b>53.32</b>	48.83	45.66	22.19	<b>13.63</b>	<b>13.48</b>	<b>11.99</b>
Nominal	46.99	46.88	45.59	38.59	10.59	10.59	10.59	10.59

Table 5: Adversarial Accuracy for CIFAR with PGD- $L_2$  attacks

natural accuracy) against attacks with  $L_1$  norm smaller or equal to  $\rho = 2.8$ . Similarly, in Table 7 we observe that for this same attacks RUB has at least 97.11% adversarial accuracy (less than 1% decrease over natural accuracy) for the MNIST data set. And finally, for the CIFAR data set, we can see in Table 8 that RUB achieves 45.66% adversarial accuracy (less than 5% decrease over natural accuracy) against attacks whose  $L_1$  norm is upper bounded by  $\rho = 5.54$ .

$\rho =$	0.00	0.01	0.06	0.28	2.80	8.40	14.00	28.00
RUB	90.27	90.16	90.35	89.49	<b>86.02</b>	<b>80.55</b>	<b>76.21</b>	<b>66.95</b>
ARUB- $L_1$	<b>90.51</b>	90.51	90.39	<b>89.73</b>	85.59	73.98	69.61	47.54
ARUB- $L_\infty$	89.96	89.92	89.84	88.75	76.60	21.37	10.16	9.84
Baseline- $L_\infty$	89.49	89.38	90.16	87.50	77.42	46.41	20.04	15.23
PGD- $L_\infty$	89.92	<b>90.74</b>	<b>90.47</b>	87.85	78.75	40.35	19.22	15.55
Nominal	88.59	88.55	88.48	87.93	77.50	40.98	15.04	9.88

Table 6: Lower Bound for the adversarial accuracy achieved for the Fashion MNIST data set with respect to uncertainty sets bounded in  $L_1$  norm by  $\rho$ .

$\rho =$	0.00	0.01	0.06	0.28	2.80	8.40	14.00	28.00
RUB	98.01	97.93	97.93	97.46	<b>97.11</b>	<b>93.67</b>	<b>89.77</b>	<b>74.96</b>
ARUB- $L_1$	<b>98.52</b>	<b>98.48</b>	<b>98.48</b>	98.20	96.48	89.96	80.86	26.05
ARUB- $L_\infty$	98.40	98.40	98.28	97.54	94.69	68.52	16.56	12.19
Baseline- $L_\infty$	98.05	98.05	98.05	97.81	95.23	57.23	20.74	10.35
PGD- $L_\infty$	98.48	<b>98.48</b>	98.44	<b>98.36</b>	95.55	63.59	15.43	11.60
Nominal	97.73	97.73	97.58	97.54	93.87	44.80	10.31	10.23

Table 7: Lower Bound for the adversarial accuracy achieved for the MNIST data set with respect to uncertainty sets bounded in  $L_1$  norm by  $\rho$ .

$\rho =$	0.00	0.01	0.06	0.55	5.54	16.63	27.71	55.43
RUB	50.62	50.62	49.96	48.91	<b>45.66</b>	<b>37.81</b>	<b>32.85</b>	<b>23.28</b>
ARUB- $L_1$	53.40	53.16	51.99	<b>51.33</b>	43.36	33.83	27.19	15.16
ARUB- $L_\infty$	53.67	53.52	53.20	47.07	37.30	14.26	9.65	9.65
Baseline- $L_\infty$	53.32	53.24	52.66	46.09	36.99	13.71	9.61	9.61
PGD- $L_\infty$	<b>54.88</b>	<b>54.80</b>	<b>53.98</b>	49.26	37.42	27.30	14.02	12.46
Nominal	46.88	46.88	46.76	44.69	37.19	14.88	9.02	8.95

Table 8: Lower Bound for the adversarial accuracy achieved for the CIFAR data set with respect to uncertainty sets bounded in  $L_1$  norm by  $\rho$ .

## 7. Conclusions

We developed two new methods for robust training of neural networks, both of which provide a new objective function in closed form solution that can be effectively trained with backpropagation. First, we found an approximated upper bound for the robust loss by incorporating the first order approximation of the network’s output layer. This method does not provide security guar-

antees against adversarial attacks but it performs very well across a variety of data sets when the uncertainty set is small. Second, by extending state-of-the-art tools from robust optimization to non-convex and non-concave functions, we were able to construct an exact upper bound for the robust counterpart of the min-max problem, thus obtaining a new robust loss than can be tractably minimized for many applications. Experimental results show that this method has a performance edge for larger uncertainty sets. Both methods run significantly faster than adversarial training, although their memory requirements increase proportionally to the dimension of the input. Lastly, we provide evidence that adding robustness can improve the natural accuracy of neural networks for classification problems with tabular or vision data.

**Code Availability Statement.** All the code to reproduce the results can be found here: <https://github.com/kimvc7/Robustness>. An illustrative example on how to use the code to train a network is provided here: <https://colab.research.google.com/github/kimvc7/Robustness/blob/main/demo.ipynb>

**Acknowledgements.** Xavier Boix has been supported by the Center for Brains, Minds and Machines (funded by NSF STC award CCF- 1231216), the R01EY020517 grant from the National Eye Institute (NIH) and Fujitsu Laboratories Ltd. (Contract No. 40008819).

## References

- Ross Anderson, Joey Huchette, Will Ma, Christian Tjandraatmadja, and Juan Pablo Vielma. Strong mixed-integer programming formulations for trained neural networks. *Mathematical Programming*, pages 1–37, 2020.
- Anish Athalye, Nicholas Carlini, and David Wagner. Obfuscated gradients give a false sense of security: Circumventing defenses to adversarial examples, 2018.
- Mislav Balunovic and Martin Vechev. Adversarial training and provable defenses: Bridging the gap. In *International Conference on Learning Representations*, 2019.
- Aharon Ben-Tal, Laurent El Ghaoui, and Arkadi Nemirovski. *Robust optimization*. Princeton university press, 2009.
- Aharon Ben-Tal, Dick Den Hertog, and Jean-Philippe Vial. Deriving robust counterparts of non-linear uncertain inequalities. *Mathematical programming*, 149(1):265–299, 2015.
- Dimitris Bertsimas and Dick den Hertog. *Robust and Adaptive Optimization*. Dynamic Ideas LLC, 2022.
- Dimitris Bertsimas, David B Brown, and Constantine Caramanis. Theory and applications of robust optimization. *SIAM Review*, 53(3):464–501, 2011.
- Dimitris Bertsimas, Jack Dunn, Colin Pawlowski, and Ying Daisy Zhuo. Robust classification. *INFORMS Journal on Optimization*, 1(1):2–34, 2019.
- Dimitris Bertsimas, Dick den Hertog, Jean Pauphilet, and Jianzhe Zhen. Robust convex optimization: A new perspective that unifies and extends. *Submitted to Mathematics of Operations Research*, 2020.

- Rudy Bunel, Ilker Turkaslan, Philip HS Torr, Pushmeet Kohli, and M Pawan Kumar. A unified view of piecewise linear neural network verification. *arXiv preprint arXiv:1711.00455*, 2017.
- André Chassein and Marc Goerigk. On the complexity of robust geometric programming with polyhedral uncertainty. *Operations Research Letters*, 47(1):21–24, 2019.
- Jeremy Cohen, Elan Rosenfeld, and Zico Kolter. Certified adversarial robustness via randomized smoothing. In *International Conference on Machine Learning*, pages 1310–1320. PMLR, 2019.
- Sumanth Dathathri, Krishnamurthy Dvijotham, Alexey Kurakin, Aditi Raghunathan, Jonathan Uesato, Rudy Bunel, Shreya Shankar, Jacob Steinhardt, Ian Goodfellow, Percy Liang, and Pushmeet Kohli. Enabling certification of verification-agnostic networks via memory-efficient semidefinite programming. *arXiv preprint arXiv:2010.11645*, 2020.
- Li Deng. The mnist database of handwritten digit images for machine learning research. *IEEE Signal Processing Magazine*, 29(6):141–142, 2012.
- Dheeru Dua and Casey Graff. UCI machine learning repository, 2017. URL <http://archive.ics.uci.edu/ml>.
- Krishnamurthy Dvijotham, Sven Gowal, Robert Stanforth, Relja Arandjelovic, Brendan O’Donoghue, Jonathan Uesato, and Pushmeet Kohli. Training verified learners with learned verifiers. *arXiv preprint arXiv:1805.10265*, 2018a.
- Krishnamurthy Dvijotham, Robert Stanforth, Sven Gowal, Timothy A Mann, and Pushmeet Kohli. A dual approach to scalable verification of deep networks. In *UAI*, volume 1, page 3, 2018b.
- Timon Gehr, Matthew Mirman, Dana Drachler-Cohen, Petar Tsankov, Swarat Chaudhuri, and Martin Vechev. Ai2: Safety and robustness certification of neural networks with abstract interpretation. In *2018 IEEE Symposium on Security and Privacy (SP)*, pages 3–18. IEEE, 2018.
- Ian J. Goodfellow, Jonathon Shlens, and Christian Szegedy. Explaining and harnessing adversarial examples, 2015.
- Sven Gowal, Krishnamurthy Dvijotham, Robert Stanforth, Rudy Bunel, Chongli Qin, Jonathan Uesato, Relja Arandjelovic, Timothy Mann, and Pushmeet Kohli. Scalable verified training for provably robust image classification. In *Proceedings of the IEEE/CVF International Conference on Computer Vision*, pages 4842–4851, 2019.
- Matthias Hein and Maksym Andriushchenko. Formal guarantees on the robustness of a classifier against adversarial manipulation. *CoRR*, abs/1705.08475, 2017. URL <http://arxiv.org/abs/1705.08475>.
- Ruitong Huang, Bing Xu, Dale Schuurmans, and Csaba Szepesvari. Learning with a strong adversary, 2016.
- Andrew Ilyas, Ajil Jalal, Eirini Asteri, Constantinos Daskalakis, and Alexandros G. Dimakis. The robust manifold defense: Adversarial training using generative models. *CoRR*, abs/1712.09196, 2017. URL <http://arxiv.org/abs/1712.09196>.
- Andrew Ilyas, Shibani Santurkar, Dimitris Tsipras, Logan Engstrom, Brandon Tran, and Aleksander Madry. Adversarial examples are not bugs, they are features. *arXiv preprint arXiv:1905.02175*, 2019.

- Vishaal Munusamy Kabilan, Brandon Morris, and Anh Nguyen. Vectordefense: Vectorization as a defense to adversarial examples. *CoRR*, abs/1804.08529, 2018. URL <http://arxiv.org/abs/1804.08529>.
- Guy Katz, Clark Barrett, David L Dill, Kyle Julian, and Mykel J Kochenderfer. Reluplex: An efficient smt solver for verifying deep neural networks. In *International Conference on Computer Aided Verification*, pages 97–117. Springer, 2017.
- Alex Krizhevsky. Learning multiple layers of features from tiny images. Technical report, 2009.
- Alexey Kurakin, Ian Goodfellow, Samy Bengio, et al. Adversarial examples in the physical world, 2016.
- Alex Lamb, Jonathan Binas, Anirudh Goyal, Dmitriy Serdyuk, Sandeep Subramanian, Ioannis Mitliagkas, and Yoshua Bengio. Fortified networks: Improving the robustness of deep networks by modeling the manifold of hidden representations. *arXiv preprint arXiv:1804.02485*, 2018.
- Mathias Lecuyer, Vaggelis Atlidakis, Roxana Geambasu, Daniel Hsu, and Suman Jana. Certified robustness to adversarial examples with differential privacy. In *2019 IEEE Symposium on Security and Privacy (SP)*, pages 656–672. IEEE, 2019.
- Aleksander Madry, Aleksandar Makelov, Ludwig Schmidt, Dimitris Tsipras, and Adrian Vladu. Towards deep learning models resistant to adversarial attacks, 2019.
- Matthew Mirman, Timon Gehr, and Martin Vechev. Differentiable abstract interpretation for provably robust neural networks. In *International Conference on Machine Learning*, pages 3578–3586. PMLR, 2018.
- Aaditya Prakash, Nick Moran, Solomon Garber, Antonella DiLillo, and James A. Storer. Deflecting adversarial attacks with pixel deflection. *CoRR*, abs/1801.08926, 2018. URL <http://arxiv.org/abs/1801.08926>.
- Aditi Raghunathan, Jacob Steinhardt, and Percy Liang. Certified defenses against adversarial examples. *arXiv preprint arXiv:1801.09344*, 2018a.
- Aditi Raghunathan, Jacob Steinhardt, and Percy Liang. Semidefinite relaxations for certifying robustness to adversarial examples. *arXiv preprint arXiv:1811.01057*, 2018b.
- Jonas Rauber, Wieland Brendel, and Matthias Bethge. Foolbox: A python toolbox to benchmark the robustness of machine learning models. In *Reliable Machine Learning in the Wild Workshop, 34th International Conference on Machine Learning*, 2017. URL <http://arxiv.org/abs/1707.04131>.
- Jonas Rauber, Roland Zimmermann, Matthias Bethge, and Wieland Brendel. Foolbox native: Fast adversarial attacks to benchmark the robustness of machine learning models in pytorch, tensorflow, and jax. *Journal of Open Source Software*, 5(53):2607, 2020. 10.21105/joss.02607. URL <https://doi.org/10.21105/joss.02607>.
- R. Tyrrell Rockafellar. *Convex analysis*. Princeton Mathematical Series. Princeton University Press, Princeton, N. J., 1970.
- Ernst Roos, Dick den Hertog, Aharon Ben-Tal, F De Ruiter, and Jianzhe Zhen. Tractable approximation of hard uncertain optimization problems. *Available on Optimization-Online*, 2020.

- Andrew Slavin Ross and Finale Doshi-Velez. Improving the adversarial robustness and interpretability of deep neural networks by regularizing their input gradients, 2017.
- Gagandeep Singh, Timon Gehr, Matthew Mirman, Markus Püschel, and Martin T Vechev. Fast and effective robustness certification. *NeurIPS*, 1(4):6, 2018.
- Christian Szegedy, Wojciech Zaremba, Ilya Sutskever, Joan Bruna, Dumitru Erhan, Ian Goodfellow, and Rob Fergus. Intriguing properties of neural networks. *arXiv preprint arXiv:1312.6199*, 2013.
- Vincent Tjeng, Kai Xiao, and Russ Tedrake. Evaluating robustness of neural networks with mixed integer programming, 2019.
- Lily Weng, Huan Zhang, Hongge Chen, Zhao Song, Cho-Jui Hsieh, Luca Daniel, Duane Boning, and Inderjit Dhillon. Towards fast computation of certified robustness for relu networks. In *International Conference on Machine Learning*, pages 5276–5285. PMLR, 2018.
- Eric Wong and Zico Kolter. Provable defenses against adversarial examples via the convex outer adversarial polytope. In *International Conference on Machine Learning*, pages 5286–5295. PMLR, 2018.
- Eric Wong, Frank R Schmidt, Jan Hendrik Metzen, and J Zico Kolter. Scaling provable adversarial defenses. *arXiv preprint arXiv:1805.12514*, 2018.
- Han Xiao, Kashif Rasul, and Roland Vollgraf. Fashion-mnist: a novel image dataset for benchmarking machine learning algorithms, 2017.
- Cihang Xie, Jianyu Wang, Zhishuai Zhang, Zhou Ren, and Alan Yuille. Mitigating adversarial effects through randomization, 2017.
- Ziang Yan, Yiwen Guo, and Changshui Zhang. Deep defense: Training dnns with improved adversarial robustness. *arXiv preprint arXiv:1803.00404*, 2018.
- Huan Zhang, Tsui-Wei Weng, Pin-Yu Chen, Cho-Jui Hsieh, and Luca Daniel. Efficient neural network robustness certification with general activation functions. *arXiv preprint arXiv:1811.00866*, 2018.
- Huan Zhang, Hongge Chen, Chaowei Xiao, Sven Gowal, Robert Stanforth, Bo Li, Duane Boning, and Cho-Jui Hsieh. Towards stable and efficient training of verifiably robust neural networks. *arXiv preprint arXiv:1906.06316*, 2019.
- Jianzhe Zhen, FJCT de Ruiter, and D Den Hertog. Robust optimization for models with uncertain soc and sdp constraints. *Optimization Online*, 2017.

## Appendix A: Proofs of Lemmas

In this Appendix, we prove lemmas 1, 2 and 3.

### A1: Proof of Lemma 1

**Proof** Since  $f$  is convex and closed, we have  $f = (f^*)^*$  (Rockafellar, 1970), and applying the definition of the convex conjugate function we obtain

$$f(\mathbf{z}(\boldsymbol{\delta})) = (f^*)^*(\mathbf{z}(\boldsymbol{\delta})) = \sup_{\mathbf{u} \in \text{dom}(f^*)} \mathbf{z}(\boldsymbol{\delta})^\top \mathbf{u} - f^*(\mathbf{u}),$$

which implies

$$\begin{aligned} \sup_{\boldsymbol{\delta} \in \mathcal{U}} f(\mathbf{z}(\boldsymbol{\delta})) + g(\mathbf{z}(\boldsymbol{\delta})) &= \sup_{\boldsymbol{\delta} \in \mathcal{U}} \sup_{\mathbf{u} \in \text{dom}(f^*)} \mathbf{z}(\boldsymbol{\delta})^\top \mathbf{u} - f^*(\mathbf{u}) + g(\mathbf{z}(\boldsymbol{\delta})) \\ &= \sup_{\mathbf{u} \in \text{dom}(f^*)} \sup_{\boldsymbol{\delta} \in \mathcal{U}} \mathbf{z}(\boldsymbol{\delta})^\top \mathbf{u} - f^*(\mathbf{u}) + g(\mathbf{z}(\boldsymbol{\delta})), \end{aligned}$$

as desired. ■

### A2: Proof of Lemma 2

Let  $\mathcal{Z} = \{\mathbf{z}(\boldsymbol{\delta}) : \boldsymbol{\delta} \in \mathcal{U}\}$ . Defining the indicator function

$$\gamma(\mathbf{z}|\mathcal{Z}) = \begin{cases} 0 & \text{if } \mathbf{z} \in \mathcal{Z}, \\ \infty & \text{otherwise,} \end{cases}$$

and applying the Fenchel duality theorem (Rockafellar, 1970), we obtain:

$$\sup_{\boldsymbol{\delta} \in \mathcal{U}} g(\mathbf{z}(\boldsymbol{\delta})) = \sup_{\mathbf{z} \in \mathcal{Z}} g(\mathbf{z}) = \sup_{\mathbf{z} \in \text{dom}(g) \cap \text{dom}(\gamma)} g(\mathbf{z}) - \gamma(\mathbf{z}|\mathcal{Z}) = \inf_{\mathbf{v} \in \text{dom}(g_*)} \gamma^*(\mathbf{v}|\mathcal{Z}) - g_*(\mathbf{v}) \quad (28)$$

Finally, since  $\gamma^*(\mathbf{v}|\mathcal{Z}) = \sup_{\mathbf{z} \in \mathcal{Z}} \mathbf{z}^\top \mathbf{v}$ , we conclude

$$\sup_{\boldsymbol{\delta} \in \mathcal{U}} g(\mathbf{z}(\boldsymbol{\delta})) = \inf_{\mathbf{v} \in \text{dom}(g_*)} \sup_{\mathbf{z} \in \mathcal{Z}} \mathbf{z}^\top \mathbf{v} - g_*(\mathbf{v}) = \inf_{\mathbf{v} \in \text{dom}(g_*)} \sup_{\boldsymbol{\delta} \in \mathcal{U}} \mathbf{z}(\boldsymbol{\delta})^\top \mathbf{v} - g_*(\mathbf{v}).$$

### A3: Proof of Lemma 3

We first prove part a). By definition, we have

$$f^*(\mathbf{z}) = \sup_{\mathbf{x}} \mathbf{z}^\top \mathbf{x} - \mathbf{p}^\top [\mathbf{x}]^+.$$

Notice that if the  $i^{\text{th}}$  component of  $\mathbf{z}$  is negative for any  $i$ , then  $f^*(\mathbf{z}) = \infty$  because  $\mathbf{x}$  can be the vector with an arbitrarily large negative value in the  $i^{\text{th}}$  coordinate and 0 everywhere else. Similarly,



if the  $i^{\text{th}}$  component of  $\mathbf{z}$  is larger than the  $i^{\text{th}}$  coordinate of  $\mathbf{p}$  for any  $i$ , then again  $f^*(\mathbf{z}) = \infty$  because  $\mathbf{x}$  can be the vector with an arbitrarily large positive value in the  $i^{\text{th}}$  coordinate and 0 everywhere else. Moreover, if  $\mathbf{0} \leq \mathbf{z} \leq \mathbf{p}$ , then

$$\sup_{\mathbf{x}} \mathbf{z}^\top \mathbf{x} - \mathbf{p}^\top [\mathbf{x}]^+ \leq \sup_{\mathbf{x}} \mathbf{z}^\top \mathbf{x} - \mathbf{z}^\top [\mathbf{x}]^+ = \sup_{\mathbf{x}} \mathbf{z}^\top (\mathbf{x} - [\mathbf{x}]^+) \leq 0.$$

Since  $\mathbf{x} = \mathbf{0}$  achieves an objective value of 0, we conclude that  $\mathbf{0} \leq \mathbf{z} \leq \mathbf{p}$  implies  $f^*(\mathbf{z}) = 0$  as desired.

Next, we proceed to prove part b). By definition of the concave conjugate we have

$$g_*(\mathbf{z}) = \inf_{\mathbf{x}} \mathbf{z}^\top \mathbf{x} - (\mathbf{x}^\top \mathbf{u} - \mathbf{q}^\top [\mathbf{x}]^+) = \inf_{\mathbf{x}} (\mathbf{z} - \mathbf{u})^\top \mathbf{x} + \mathbf{q}^\top [\mathbf{x}]^+.$$

If the  $i^{\text{th}}$  component of  $\mathbf{z}$  is larger than the  $i^{\text{th}}$  component of  $\mathbf{u}$  for any  $i$ , then  $g_*(\mathbf{z}) = \infty$  because  $\mathbf{x}$  can be the vector with an arbitrarily large negative value in the  $i^{\text{th}}$  coordinate and 0 everywhere else. Similarly, if the  $i^{\text{th}}$  component of  $\mathbf{z}$  is smaller than the  $i^{\text{th}}$  coordinate of  $(\mathbf{u} - \mathbf{q})$  for any  $i$ , then again  $g_*(\mathbf{z}) = \infty$  because  $\mathbf{x}$  can be the vector with an arbitrarily large positive value in the  $i^{\text{th}}$  coordinate and 0 everywhere else. In addition, if  $\mathbf{u} - \mathbf{q} \leq \mathbf{z} \leq \mathbf{u}$ , then

$$\inf_{\mathbf{x}} (\mathbf{z} - \mathbf{u})^\top \mathbf{x} + \mathbf{q}^\top [\mathbf{x}]^+ \geq \inf_{\mathbf{x}} (\mathbf{z} - \mathbf{u})^\top \mathbf{x} + (\mathbf{u} - \mathbf{z})^\top [\mathbf{x}]^+ = \inf_{\mathbf{x}} (\mathbf{u} - \mathbf{z})^\top ([\mathbf{x}]^+ - \mathbf{x}) \geq 0.$$

Since  $\mathbf{x} = \mathbf{0}$  achieves an objective value of 0, we conclude that  $\mathbf{u} - \mathbf{q} \leq \mathbf{z} \leq \mathbf{u}$  implies  $g_*(\mathbf{z}) = 0$  as desired.

## Appendix B: Generalized Results

We now state and proof the generalization of Theorem 4, Corollary 5 and Theorem 6 for the case in which the neural network has more than 2 layers.

### Theorem 7 (Generalization of Theorem 4)

For all  $2 \leq l \leq L$ , it holds

$$\begin{aligned} \sup_{\delta \in \mathcal{U}} \mathbf{c}_k^\top \mathbf{z}^\ell(\theta, \mathbf{x} + \delta) = & \tag{29} \\ \sup_{\mathbf{s}_L} \inf_{\mathbf{t}_L} \dots \sup_{\mathbf{s}_l} \inf_{\mathbf{t}_l} \sup_{\delta \in \mathcal{U}} & (\mathbf{p}_l - \mathbf{q}_l)^\top \mathbf{z}^{l-1}(\theta, \mathbf{x} + \delta) + \sum_{\ell=l}^{L-1} (\mathbf{p}_{\ell+1} - \mathbf{q}_{\ell+1})^\top \mathbf{b}^\ell + \mathbf{c}_k^\top \mathbf{b}^L \\ \text{s.t. } \mathbf{p}_L = & [(\mathbf{W}^L)^\top \mathbf{c}_k]^+ \odot \mathbf{s}_L \\ \mathbf{q}_L = & [-(\mathbf{W}^L)^\top \mathbf{c}_k]^+ \odot \mathbf{t}_L \\ \mathbf{p}_\ell = & (([\mathbf{W}^\ell]^+)^\top \mathbf{p}_{\ell+1} + ([-\mathbf{W}^\ell]^+)^\top \mathbf{q}_{\ell+1}) \odot \mathbf{s}_\ell \quad \forall \ell = l, \dots, L-1 \\ \mathbf{q}_\ell = & (([-\mathbf{W}^\ell]^+)^\top \mathbf{p}_{\ell+1} + ([\mathbf{W}^\ell]^+)^\top \mathbf{q}_{\ell+1}) \odot \mathbf{t}_\ell \quad \forall \ell = l, \dots, L-1 \\ 0 \leq \mathbf{s}_\ell, \mathbf{t}_\ell \leq 1 & \quad \forall \ell = l, \dots, L. \end{aligned} \tag{30}$$

**Proof** We will proceed by backward induction on the layer number  $l$ .

**Case  $l = L$ :**

The proof is equivalent to the case  $L = 2$  already proved in Section 5.

**Case  $l - 1$ :**

Suppose the theorem holds for some fixed  $l$  with  $l > 2$ . We have

$$\begin{aligned} & (\mathbf{p}_l - \mathbf{q}_l)^\top \mathbf{z}^{l-1}(\theta, \mathbf{x} + \delta) \\ &= (\mathbf{p}_l - \mathbf{q}_l)^\top (\mathbf{W}^{l-1} [\mathbf{z}^{l-2}(\theta, \mathbf{x} + \delta)]^+ + \mathbf{b}^{l-1}) \\ &= f_+(\mathbf{z}^{l-2}(\theta, \mathbf{x} + \delta)) - f_-(\mathbf{z}^{l-2}(\theta, \mathbf{x} + \delta)) + (\mathbf{p}_l - \mathbf{q}_l)^\top \mathbf{b}^{l-1}, \end{aligned}$$

where

$$\begin{aligned} f_+(\mathbf{x}) &= (\mathbf{p}_l^\top [\mathbf{W}^{l-1}]^+ + \mathbf{q}_l^\top [-\mathbf{W}^{l-1}]^+) [\mathbf{x}]^+, \quad \text{and} \\ f_-(\mathbf{x}) &= (\mathbf{p}_l^\top [-\mathbf{W}^{l-1}]^+ + \mathbf{q}_l^\top [\mathbf{W}^{l-1}]^+) [\mathbf{x}]^+. \end{aligned}$$

By Lemma 1 we then obtain

$$\begin{aligned} & \sup_{\delta \in \mathcal{U}} (\mathbf{p}_l - \mathbf{q}_l)^\top \mathbf{z}^{l-1}(\theta, \mathbf{x} + \delta) \\ &= \sup_{\delta \in \mathcal{U}} f_+(\mathbf{z}^{l-2}(\theta, \mathbf{x} + \delta)) - f_-(\mathbf{z}^{l-2}(\theta, \mathbf{x} + \delta)) + (\mathbf{p}_l - \mathbf{q}_l)^\top \mathbf{b}^{l-1} \\ &= \sup_{\mathbf{u}_{l-1} \in \text{dom}(f_+^*)} \sup_{\delta \in \mathcal{U}} \mathbf{u}_{l-1}^\top \mathbf{z}^{l-2}(\theta, \mathbf{x} + \delta) - f_-(\mathbf{z}^{l-2}(\theta, \mathbf{x} + \delta)) + (\mathbf{p}_l - \mathbf{q}_l)^\top \mathbf{b}^{l-1}. \end{aligned}$$

Defining the concave function  $g(\mathbf{x}) = \mathbf{u}_{l-1}^\top \mathbf{x} - f_-(\mathbf{x})$ , and applying Lemma 2 we obtain

$$\sup_{\delta \in \mathcal{U}} (\mathbf{p}_l - \mathbf{q}_l)^\top \mathbf{z}^{l-1}(\theta, \mathbf{x} + \delta) \quad (31)$$

$$= \sup_{\mathbf{u}_{l-1} \in \text{dom}(f_+^*)} \inf_{\mathbf{v}_{l-1} \in \text{dom}(g^*)} \sup_{\delta \in \mathcal{U}} \mathbf{v}_{l-1}^\top \mathbf{z}^{l-2}(\theta, \mathbf{x} + \delta) + (\mathbf{p}_l - \mathbf{q}_l)^\top \mathbf{b}^{l-1}. \quad (32)$$

Lastly, by Lemma 3 we can substitute

$$\begin{aligned} \mathbf{u}_{l-1} &= ((\mathbf{W}^{l-1})^+)^\top \mathbf{p}_l + ([-\mathbf{W}^{l-1}]^+)^\top \mathbf{q}_l \odot \mathbf{s}_{l-1} \\ &= \mathbf{p}_{l-1}, \quad \text{and} \\ \mathbf{v}_{l-1} &= ((\mathbf{W}^{l-1})^+)^\top \mathbf{p}_l + ([-\mathbf{W}^{l-1}]^+)^\top \mathbf{q}_l \odot \mathbf{s}_{l-1} - (\mathbf{p}_l[-\mathbf{W}^{l-1}]^+ + \mathbf{q}_l[\mathbf{W}^{l-1}]^+) \odot \mathbf{t}_{l-1} \\ &= \mathbf{p}_{l-1} - \mathbf{q}_{l-1}, \end{aligned}$$

which together with the induction hypothesis imply that Problem (30) is equivalent to

$$\begin{aligned} \sup_{\delta \in \mathcal{U}} \mathbf{c}_k^\top \mathbf{z}^{\ell-1}(\theta, \mathbf{x} + \delta) = \\ \sup_{\mathbf{s}_L} \inf_{\mathbf{t}_L} \dots \sup_{\mathbf{s}_{l-1}} \inf_{\mathbf{t}_{l-1}} \sup_{\delta \in \mathcal{U}} (\mathbf{p}_{l-1} - \mathbf{q}_{l-1})^\top \mathbf{z}^{l-2}(\theta, \mathbf{x} + \delta) + \sum_{\ell=l-1}^{L-1} (\mathbf{p}_{\ell+1} - \mathbf{q}_{\ell+1})^\top \mathbf{b}^\ell + \mathbf{c}_k^\top \mathbf{b}^L \\ \text{s.t. } \mathbf{p}_L = [(\mathbf{W}^L)^\top \mathbf{c}_k]^+ \odot \mathbf{s}_L \\ \mathbf{q}_L = [-\mathbf{W}^L]^\top \mathbf{c}_k]^+ \odot \mathbf{t}_L \\ \mathbf{p}_\ell = (([\mathbf{W}^\ell]^+)^\top \mathbf{p}_{\ell+1} + ([-\mathbf{W}^\ell]^+)^\top \mathbf{q}_{\ell+1}) \odot \mathbf{s}_\ell \quad \forall l-1 \leq \ell \leq L-1 \\ \mathbf{q}_\ell = (([-\mathbf{W}^\ell]^+)^\top \mathbf{p}_{\ell+1} + ([\mathbf{W}^\ell]^+)^\top \mathbf{q}_{\ell+1}) \odot \mathbf{t}_\ell \quad \forall l-1 \leq \ell \leq L-1 \\ 0 \leq \mathbf{s}_\ell, \mathbf{t}_\ell \leq 1 \quad \forall \ell = l-1, \dots, L, \end{aligned}$$

and therefore the theorem holds for  $l-1$  as desired.  $\blacksquare$

### Corollary 8 (Generalization of Corollary 5)

If  $\mathcal{U} = \{\delta : \|\delta\|_p \leq \rho\}$ , then:

$$\begin{aligned} \sup_{\delta \in \mathcal{U}} \mathbf{c}_k^\top \mathbf{z}^L(\theta, \mathbf{x} + \delta) \quad (33) \\ = \sup_{\mathbf{s}_L} \inf_{\mathbf{t}_L} \dots \sup_{\mathbf{s}_2} \inf_{\mathbf{t}_2} \rho \|(\mathbf{p}_2 - \mathbf{q}_2)^\top \mathbf{W}^1\|_q + (\mathbf{p}_2 - \mathbf{q}_2)^\top \mathbf{W}^1 \mathbf{x} + \sum_{\ell=1}^{L-1} (\mathbf{p}_{\ell+1} - \mathbf{q}_{\ell+1})^\top \mathbf{b}^\ell + \mathbf{c}_k^\top \mathbf{b}^L \\ \text{s.t. } \mathbf{p}_L = [(\mathbf{W}^L)^\top \mathbf{c}_k]^+ \odot \mathbf{s}_L \\ \mathbf{q}_L = [-\mathbf{W}^L]^\top \mathbf{c}_k]^+ \odot \mathbf{t}_L \\ \mathbf{p}_\ell = (([\mathbf{W}^\ell]^+)^\top \mathbf{p}_{\ell+1} + ([-\mathbf{W}^\ell]^+)^\top \mathbf{q}_{\ell+1}) \odot \mathbf{s}_\ell \quad \forall \ell = 2, \dots, L-1 \\ \mathbf{q}_\ell = (([-\mathbf{W}^\ell]^+)^\top \mathbf{p}_{\ell+1} + ([\mathbf{W}^\ell]^+)^\top \mathbf{q}_{\ell+1}) \odot \mathbf{t}_\ell \quad \forall \ell = 2, \dots, L-1 \\ 0 \leq \mathbf{s}_\ell, \mathbf{t}_\ell \leq 1 \quad \forall \ell = 2, \dots, L, \end{aligned} \quad (34)$$

where  $\|\cdot\|_q$  is the conjugate norm of  $\|\cdot\|_p$ .

**Proof** The proof follows directly after applying Theorem 7 with  $l = 2$  and using again Eq. (23).  
 ■

**Definition 9** We introduce the following definitions to simplify notation:

$$\begin{aligned}
 \mathbf{s} &:= (\mathbf{s}_2, \dots, \mathbf{s}_L) \\
 \mathbf{t} &:= (\mathbf{t}_2, \dots, \mathbf{t}_L) \\
 \mathbf{p}_L(\mathbf{s}, \mathbf{t}) &:= [(\mathbf{W}^2)^\top \mathbf{c}_k]^+ \odot \mathbf{s}_L \\
 \mathbf{q}_L(\mathbf{s}, \mathbf{t}) &:= [-(\mathbf{W}^2)^\top \mathbf{c}_k]^+ \odot \mathbf{t}_L \\
 \\ 
 \mathbf{p}_\ell(\mathbf{s}, \mathbf{t}) &:= \left( ([\mathbf{W}^\ell]^+)^\top \mathbf{p}_{\ell+1}(\mathbf{s}, \mathbf{t}) + [(-\mathbf{W}^\ell)^+]^\top \mathbf{q}_{\ell+1}(\mathbf{s}, \mathbf{t}) \right) \odot \mathbf{s}_\ell \quad \forall 1 \leq \ell < L \\
 \mathbf{q}_\ell(\mathbf{s}, \mathbf{t}) &:= \left( [(-\mathbf{W}^\ell)^+]^\top \mathbf{p}_{\ell+1}(\mathbf{s}, \mathbf{t}) + ([\mathbf{W}^\ell]^+)^\top \mathbf{q}_{\ell+1}(\mathbf{s}, \mathbf{t}) \right) \odot \mathbf{t}_\ell \quad \forall 1 \leq \ell < L \\
 \\ 
 R_\ell(\mathbf{s}, \mathbf{t}) &:= \sum_{\ell'=\ell}^{L-1} (\mathbf{p}_{\ell'+1}(\mathbf{s}, \mathbf{t}) - \mathbf{q}_{\ell'+1}(\mathbf{s}, \mathbf{t}))^\top \mathbf{b}^{\ell'}.
 \end{aligned}$$

**Theorem 10 (Generalization of Theorem 6)**

$$\begin{aligned}
 &\sup_{\boldsymbol{\delta}: \|\boldsymbol{\delta}\|_1 \leq \rho} \mathbf{c}_k^\top \mathbf{z}^L(\theta, \mathbf{x} + \boldsymbol{\delta}) \\
 &\leq \inf_{0 \leq t \leq 1} \max_{m \in [M]} \max \left\{ g_{k,m}^L(\theta, \mathbf{x}, \mathbf{t}, \rho), g_{k,m}^L(\theta, \mathbf{x}, \mathbf{t}, -\rho) \right\}, \tag{35}
 \end{aligned}$$

where the new network  $g$  is defined by the equations

$$\begin{aligned}
 g_m^1(\mathbf{W}, \mathbf{x}, \mathbf{t}, a, r) &= r(a\mathbf{W}_m^1 + \mathbf{W}^1 \mathbf{x} + \mathbf{b}^1) \\
 g_m^\ell(\theta, \mathbf{x}, \mathbf{t}, a, r) &= [r\mathbf{W}^\ell]^+ [g_m^{\ell-1}(\mathbf{W}, \mathbf{x}, \mathbf{t}, a, 1)]^+ + [-r\mathbf{W}^\ell]^+ [g_m^{\ell-1}(\mathbf{W}, \mathbf{x}, \mathbf{t}, a, -1)] \odot \mathbf{t}_\ell + r\mathbf{b}^\ell \\
 g_{k,m}^L(\theta, \mathbf{x}, \mathbf{t}, a) &= [\mathbf{c}_k^\top \mathbf{W}^L]^+ [g_m^{L-1}(\theta, \mathbf{x}, \mathbf{t}, a, 1)]^+ + [-\mathbf{c}_k^\top \mathbf{W}^L]^+ [g_m^{L-1}(\theta, \mathbf{x}, \mathbf{t}, a, -1)] \odot \mathbf{t}_L + \mathbf{c}_k^\top \mathbf{b}^L,
 \end{aligned}$$

for all  $1 < \ell < L$ ,  $1 \leq k \leq K$ ,  $a \in \{\rho, -\rho\}$ , and  $r \in \{-1, 1\}$ .

The proof of this theorem relies on the following lemma.

**Lemma 11** For all  $2 \leq \ell \leq L - 1$  it holds

$$\sup_{0 \leq s_\ell \leq 1} \mathbf{p}_\ell(\mathbf{s}, \mathbf{t})^\top g_m^{\ell-1}(\theta, \mathbf{x}, \mathbf{t}, a, 1) + \mathbf{q}_\ell(\mathbf{s}, \mathbf{t})^\top g_m^{\ell-1}(\theta, \mathbf{x}, \mathbf{t}, a, -1) \tag{36}$$

$$= \mathbf{p}_{\ell+1}(\mathbf{s}, \mathbf{t})^\top g_m^\ell(\theta, \mathbf{x}, \mathbf{t}, a, 1) + \mathbf{q}_{\ell+1}(\mathbf{s}, \mathbf{t})^\top g_m^\ell(\theta, \mathbf{x}, \mathbf{t}, a, -1) - (\mathbf{p}_{\ell+1}(\mathbf{s}, \mathbf{t}) - \mathbf{q}_{\ell+1}(\mathbf{s}, \mathbf{t}))^\top \mathbf{b}^\ell. \tag{37}$$

**Proof** Let  $2 \leq \ell \leq L - 1$ , we have

$$\begin{aligned}
 & \sup_{0 \leq s_\ell \leq 1} \mathbf{p}_\ell(\mathbf{s}, \mathbf{t})^\top g_m^{\ell-1}(\theta, \mathbf{x}, \mathbf{t}, a, 1) + \mathbf{q}_\ell(\mathbf{s}, \mathbf{t})^\top g_m^{\ell-1}(\theta, \mathbf{x}, \mathbf{t}, a, -1) \\
 &= \sup_{0 \leq s_\ell \leq 1} \left( \left( ([\mathbf{W}^\ell]^+)^{\top} \mathbf{p}_{\ell+1}(\mathbf{s}, \mathbf{t}) + ([-\mathbf{W}^\ell]^+)^{\top} \mathbf{q}_{\ell+1}(\mathbf{s}, \mathbf{t}) \right) \odot \mathbf{s}_\ell \right)^\top g_m^{\ell-1}(\theta, \mathbf{x}, \mathbf{t}, a, 1) + \\
 & \quad \left( \left( ([-\mathbf{W}^\ell]^+)^{\top} \mathbf{p}_{\ell+1}(\mathbf{s}, \mathbf{t}) + ([\mathbf{W}^\ell]^+)^{\top} \mathbf{q}_{\ell+1}(\mathbf{s}, \mathbf{t}) \right) \odot \mathbf{t}_\ell \right)^\top g_m^{\ell-1}(\theta, \mathbf{x}, \mathbf{t}, a, -1) \\
 &= \sup_{0 \leq s_\ell \leq 1} \left( \left( ([\mathbf{W}^\ell]^+)^{\top} \mathbf{p}_{\ell+1}(\mathbf{s}, \mathbf{t}) + ([-\mathbf{W}^\ell]^+)^{\top} \mathbf{q}_{\ell+1}(\mathbf{s}, \mathbf{t}) \right)^\top \left( g_m^{\ell-1}(\theta, \mathbf{x}, \mathbf{t}, a, 1) \odot \mathbf{s}_\ell \right) + \right. \\
 & \quad \left. \left( ([-\mathbf{W}^\ell]^+)^{\top} \mathbf{p}_{\ell+1}(\mathbf{s}, \mathbf{t}) + ([\mathbf{W}^\ell]^+)^{\top} \mathbf{q}_{\ell+1}(\mathbf{s}, \mathbf{t}) \right)^\top \left( g_m^{\ell-1}(\theta, \mathbf{x}, \mathbf{t}, a, -1) \odot \mathbf{t}_\ell \right) \right) \\
 &= \left( ([\mathbf{W}^\ell]^+)^{\top} \mathbf{p}_{\ell+1}(\mathbf{s}, \mathbf{t}) + ([-\mathbf{W}^\ell]^+)^{\top} \mathbf{q}_{\ell+1}(\mathbf{s}, \mathbf{t}) \right)^\top [g_m^{\ell-1}(\theta, \mathbf{x}, \mathbf{t}, a, 1)]^+ + \\
 & \quad \left( ([-\mathbf{W}^\ell]^+)^{\top} \mathbf{p}_{\ell+1}(\mathbf{s}, \mathbf{t}) + ([\mathbf{W}^\ell]^+)^{\top} \mathbf{q}_{\ell+1}(\mathbf{s}, \mathbf{t}) \right)^\top \left( g_m^{\ell-1}(\theta, \mathbf{x}, \mathbf{t}, a, -1) \odot \mathbf{t}_\ell \right) \\
 &= \mathbf{p}_{\ell+1}(\mathbf{s}, \mathbf{t})^\top g_m^\ell(\theta, \mathbf{x}, \mathbf{t}, a, 1) + \mathbf{q}_{\ell+1}(\mathbf{s}, \mathbf{t})^\top g_m^\ell(\theta, \mathbf{x}, \mathbf{t}, a, -1) - (\mathbf{p}_{\ell+1}(\mathbf{s}, \mathbf{t}) - \mathbf{q}_{\ell+1}(\mathbf{s}, \mathbf{t}))^\top \mathbf{b}^\ell,
 \end{aligned}$$

as desired. ■

**Proof** [Proof of theorem 10]

By Corollary 8 with  $p = 1$  we know

$$\sup_{\delta: \|\delta\|_1 \leq \rho} \mathbf{c}_k^\top (\mathbf{z}^L(\theta, \mathbf{x} + \delta) - \mathbf{b}^L) \tag{38}$$

$$\leq \sup_{s_L} \inf_{t_L} \dots \sup_{s_2} \inf_{t_2} \rho \|(\mathbf{p}_2(\mathbf{s}, \mathbf{t}) - \mathbf{q}_2(\mathbf{s}, \mathbf{t}))^\top \mathbf{W}^1\|_\infty + (\mathbf{p}_2(\mathbf{s}, \mathbf{t}) - \mathbf{q}_2(\mathbf{s}, \mathbf{t}))^\top \mathbf{W}^1 \mathbf{x} + R_1(\mathbf{s}, \mathbf{t}) \tag{39}$$

$$\leq \inf_{t_L \dots t_2} \sup_{s_L \dots s_2} \rho \|(\mathbf{p}_2(\mathbf{s}, \mathbf{t}) - \mathbf{q}_2(\mathbf{s}, \mathbf{t}))^\top \mathbf{W}^1\|_\infty + (\mathbf{p}_2(\mathbf{s}, \mathbf{t}) - \mathbf{q}_2(\mathbf{s}, \mathbf{t}))^\top \mathbf{W}^1 \mathbf{x} + R_1(\mathbf{s}, \mathbf{t}), \tag{40}$$

where the last inequality follows from the min-max inequality. Observe that  $\mathbf{p}_{\ell'}(\mathbf{s}, \mathbf{t})$  and  $\mathbf{q}_{\ell'}(\mathbf{s}, \mathbf{t})$  are independent on  $s_\ell$  for all  $\ell' > \ell$ , which in turn implies that  $R_{\ell'}(\mathbf{s}, \mathbf{t})$  does not depend on  $s_\ell$  for all  $\ell' > \ell$ . We can then solve the optimization problem in Eq. (34) for fixed  $\mathbf{t}$  as follows:

$$\begin{aligned}
& \sup_{0 \leq s_L, \dots, s_2 \leq 1} \rho \|(\mathbf{p}_2(\mathbf{s}, \mathbf{t}) - \mathbf{q}_2(\mathbf{s}, \mathbf{t}))^\top \mathbf{W}^1\|_\infty + (\mathbf{p}_2(\mathbf{s}, \mathbf{t}) - \mathbf{q}_2(\mathbf{s}, \mathbf{t}))^\top \mathbf{W}^1 \mathbf{x} + R_1(\mathbf{s}, \mathbf{t}) \\
&= \max_{m \in [M]} \max \left\{ \sup_{0 \leq s_L, \dots, s_2 \leq 1} (\mathbf{p}_2(\mathbf{s}, \mathbf{t}) - \mathbf{q}_2(\mathbf{s}, \mathbf{t}))^\top (\mathbf{W}^1(\mathbf{x} + \rho \mathbf{e}_m) + \mathbf{b}^1) + R_2(\mathbf{s}, \mathbf{t}), \right. \\
&\quad \left. \sup_{0 \leq s_L, \dots, s_2 \leq 1} (\mathbf{p}_2(\mathbf{s}, \mathbf{t}) - \mathbf{q}_2(\mathbf{s}, \mathbf{t}))^\top (\mathbf{W}^1(\mathbf{x} - \rho \mathbf{e}_m) + \mathbf{b}^1) + R_2(\mathbf{s}, \mathbf{t}) \right\} \\
&= \max_{m \in [M]} \max \left\{ \sup_{0 \leq s_L, \dots, s_2 \leq 1} \mathbf{p}_2(\mathbf{s}, \mathbf{t})^\top g_m^1(\theta, \mathbf{x}, \mathbf{t}, \rho, 1) + \mathbf{q}_2(\mathbf{s}, \mathbf{t})^\top g_m^1(\theta, \mathbf{x}, \mathbf{t}, \rho, -1) + R_2(\mathbf{s}, \mathbf{t}), \right. \\
&\quad \left. \sup_{0 \leq s_L, \dots, s_2 \leq 1} \mathbf{p}_2(\mathbf{s}, \mathbf{t})^\top g_m^1(\theta, \mathbf{x}, \mathbf{t}, -\rho, 1) + \mathbf{q}_2(\mathbf{s}, \mathbf{t})^\top g_m^1(\theta, \mathbf{x}, \mathbf{t}, -\rho, -1) + R_2(\mathbf{s}, \mathbf{t}) \right\}.
\end{aligned}$$

By repeatedly applying Lemma 11 for each  $\ell = 2, \dots, L-1$  we obtain

$$\begin{aligned}
& \sup_{0 \leq s_L, \dots, s_2 \leq 1} \rho \|(\mathbf{p}_2(\mathbf{s}, \mathbf{t}) - \mathbf{q}_2(\mathbf{s}, \mathbf{t}))^\top \mathbf{W}^1\|_\infty + (\mathbf{p}_2(\mathbf{s}, \mathbf{t}) - \mathbf{q}_2(\mathbf{s}, \mathbf{t}))^\top \mathbf{W}^1 \mathbf{x} + R_1(\mathbf{s}, \mathbf{t}) \\
&= \max_{m \in [M]} \max \left\{ \sup_{0 \leq s_L \leq 1} \mathbf{p}_L(\mathbf{s}, \mathbf{t})^\top g_m^{L-1}(\theta, \mathbf{x}, \mathbf{t}, \rho, 1) + \mathbf{q}_L(\mathbf{s}, \mathbf{t})^\top g_m^{L-1}(\theta, \mathbf{x}, \mathbf{t}, \rho, -1), \right. \\
&\quad \left. \sup_{0 \leq s_L \leq 1} \mathbf{p}_L(\mathbf{s}, \mathbf{t})^\top g_m^{L-1}(\theta, \mathbf{x}, \mathbf{t}, -\rho, 1) + \mathbf{q}_L(\mathbf{s}, \mathbf{t})^\top g_m^{L-1}(\theta, \mathbf{x}, \mathbf{t}, -\rho, -1) \right\} \\
&= \max_{m \in [M]} \max \left\{ \sup_{0 \leq s_L \leq 1} [\mathbf{c}_k^\top \mathbf{W}^L]^+(g_m^{L-1}(\theta, \mathbf{x}, \mathbf{t}, \rho, 1) \odot \mathbf{s}_L) + [-\mathbf{c}_k^\top \mathbf{W}^L]^+(g_m^{L-1}(\theta, \mathbf{x}, \mathbf{t}, \rho, -1) \odot \mathbf{t}_L), \right. \\
&\quad \left. \sup_{0 \leq s_L \leq 1} [\mathbf{c}_k^\top \mathbf{W}^L]^+(g_m^{L-1}(\theta, \mathbf{x}, \mathbf{t}, -\rho, 1) \odot \mathbf{s}_L) + [-\mathbf{c}_k^\top \mathbf{W}^L]^+(g_m^{L-1}(\theta, \mathbf{x}, \mathbf{t}, -\rho, -1) \odot \mathbf{t}_L) \right\} \\
&= \max_{m \in [M]} \max \left\{ g_{k,m}^L(\theta, \mathbf{x}, \mathbf{t}, \rho), g_{k,m}^L(\theta, \mathbf{x}, \mathbf{t}, -\rho) \right\} - \mathbf{c}_k^\top \mathbf{b}^L,
\end{aligned}$$

as desired. ■

## Appendix C: Other Adversarial Attacks for Vision Data Sets

In this section we further analyze adversarial accuracies with respect to the vision data sets by evaluating other types of attacks. More specifically, we show the adversarial accuracies of each method with respect to PGD attacks bounded in  $L_1$  and  $L_\infty$  norms. Across the three data sets (Fashion MNIST, MNIST and CIFAR), we observe similar trends as those obtained with  $L_2$  norm bounded attacks in Section 6.3.

$\rho =$	0.00	0.01	0.06	0.28	2.80	8.40	14.00	28.00
RUB	90.27	90.20	90.16	90.27	88.36	86.25	84.18	76.25
ARUB- $L_1$	<b>90.51</b>	<b>90.51</b>	90.43	90.35	<b>89.02</b>	<b>86.52</b>	<b>84.34</b>	<b>79.41</b>
ARUB- $L_\infty$	89.96	89.96	89.92	89.84	88.44	84.69	81.41	74.30
Baseline- $L_\infty$	89.49	89.49	90.31	89.80	87.93	84.26	80.23	70.94
PGD- $L_\infty$	89.92	89.84	<b>90.78</b>	<b>90.55</b>	88.52	85.35	83.95	75.20
Nominal	88.59	88.59	88.55	88.52	87.50	84.02	80.70	71.33

Table 9: Adversarial Accuracy for Fashion MNIST with PGD- $L_1$  attacks.

$\rho =$	0.00	0.01	0.06	0.28	2.80	8.40	14.00	28.00
RUB	98.01	97.97	97.93	97.89	97.30	97.19	96.25	93.32
ARUB- $L_1$	<b>98.52</b>	<b>98.52</b>	<b>98.48</b>	<b>98.48</b>	98.05	97.50	96.52	94.92
ARUB- $L_\infty$	98.40	98.40	98.40	98.24	<b>98.32</b>	<b>97.85</b>	97.11	94.53
Baseline- $L_\infty$	98.05	98.05	98.05	98.05	97.58	96.52	95.55	92.30
PGD- $L_\infty$	98.48	98.48	<b>98.48</b>	98.44	98.28	97.73	<b>97.30</b>	<b>95.00</b>
Nominal	97.73	97.73	97.73	97.54	97.30	95.94	94.49	90.94

Table 10: Adversarial Accuracy for MNIST with PGD- $L_1$  attacks.

$\rho =$	0.00	0.01	0.06	0.55	5.54	16.63	27.71	55.43
RUB	53.59	53.59	53.59	50.94	<b>51.33</b>	48.28	45.94	41.33
ARUB- $L_1$	53.40	53.32	53.09	51.95	50.90	<b>48.87</b>	<b>46.60</b>	41.37
ARUB- $L_\infty$	53.67	53.63	53.52	52.97	45.51	42.19	40.62	37.38
Baseline- $L_\infty$	53.32	53.28	53.24	51.17	43.01	41.29	37.77	28.83
PGD- $L_\infty$	<b>54.88</b>	<b>54.88</b>	<b>54.80</b>	<b>53.71</b>	48.91	47.15	45.70	<b>41.60</b>
Nominal	46.88	46.88	46.88	46.52	43.91	40.51	37.46	29.73

Table 11: Adversarial Accuracy for CIFAR with PGD- $L_1$  attacks.

$\rho =$	0.000	0.001	0.003	0.010	0.100	0.300	0.500	1.000
RUB	89.38	89.18	88.71	87.15	66.48	56.17	56.13	<b>55.78</b>
ARUB- $L_1$	<b>90.00</b>	<b>89.77</b>	<b>89.22</b>	87.27	67.07	31.05	11.02	9.84
ARUB- $L_\infty$	89.77	89.22	88.87	86.76	80.43	67.93	54.49	12.15
Baseline- $L_\infty$	<b>90.00</b>	88.79	87.93	85.59	56.80	30.20	29.06	27.19
PGD- $L_\infty$	89.02	89.18	88.24	<b>87.77</b>	<b>80.82</b>	<b>73.09</b>	<b>65.74</b>	31.21
Nominal	88.16	87.97	87.30	86.05	58.32	21.80	18.79	16.37

Table 12: Adversarial Accuracy for Fashion MNIST with PGD- $L_\infty$  attacks.

$\rho =$	0.000	0.001	0.003	0.010	0.100	0.300	0.500	1.000
RUB	98.52	98.36	98.32	98.36	86.09	68.52	67.15	61.56
ARUB- $L_1$	<b>99.14</b>	<b>99.02</b>	<b>98.87</b>	98.44	87.97	61.88	59.61	54.77
ARUB- $L_\infty$	98.91	98.83	98.71	<b>98.79</b>	97.42	91.52	80.98	49.69
Baseline- $L_\infty$	98.59	98.09	98.63	97.66	84.69	65.08	63.24	59.49
PGD- $L_\infty$	98.71	98.87	98.83	98.75	<b>97.66</b>	<b>93.83</b>	<b>86.80</b>	<b>64.57</b>
Nominal	98.05	97.97	97.85	97.30	81.91	23.28	18.98	17.38

Table 13: Adversarial Accuracy for MNIST with PGD- $L_\infty$  attacks.

$\rho =$	0.000	0.001	0.003	0.010	0.100	0.300	0.500	1.000
RUB	50.86	46.02	48.05	45.94	21.64	10.62	10.62	10.62
ARUB- $L_1$	53.28	51.48	<b>50.55</b>	<b>47.77</b>	27.19	10.66	10.12	10.12
ARUB- $L_\infty$	<b>55.43</b>	51.21	45.66	42.70	<b>29.61</b>	10.43	11.17	11.05
Baseline- $L_\infty$	51.48	47.54	41.56	39.22	9.92	9.92	9.92	9.92
PGD- $L_\infty$	54.49	<b>51.60</b>	48.05	46.33	25.31	<b>16.09</b>	<b>12.93</b>	<b>12.89</b>
Nominal	49.26	46.17	43.44	39.18	9.92	9.92	9.92	9.92

Table 14: Adversarial Accuracy for CIFAR with PGD- $L_\infty$  attacks.



## Appendix D: Convolutional Neural Networks

While in this paper we only consider feed forward neural networks, it is possible to extend our results to convolutional neural networks that use ReLU and MaxPool activation functions. In fact, Lemma 3 can be modified as follows:

**Lemma 12** *Let  $x \in \mathbb{R}^{A \times B}$ . Define  $MP(x) \in \mathbb{R}^{C \times D}$  as the MaxPool function whose  $(c, d)$  coordinate corresponds to  $\max_{i \in I_{cd}} \{x_i\}$  for fixed sets of indices  $I_{cd}$ , and denote by  $\otimes$  the convolution operation. If  $\mathbf{u} \in \mathbb{R}^{A \times B}$ ,  $\mathbf{p}, \mathbf{q} \in \mathbb{R}^{C \times D}$  have all nonnegative coordinates, then the functions  $f(\mathbf{x}) = \mathbf{p} \otimes MP[\mathbf{x}]^+$  and  $g(\mathbf{x}) = \mathbf{x} \otimes \mathbf{u} - \mathbf{q} \otimes MP[\mathbf{x}]^+$  satisfy*

$$\begin{aligned}
 a) f^*(z) &= \begin{cases} 0 & \text{if } 0 \leq \sum_{i \in I_{cd}} z_i \leq p_{cd}, \forall c \in [C], d \in [D], \\ \infty & \text{otherwise,} \end{cases} \quad \text{and} \\
 b) g_*(z) &= \begin{cases} 0 & \text{if } u_{cd} - q_{cd} \leq \sum_{i \in I_{cd}} z_i \leq u_{cd}, \forall c \in [C], d \in [D], \\ -\infty & \text{otherwise.} \end{cases}
 \end{aligned}$$

The lemma above allows to obtain an upper bound for the robust loss of convolutional networks with a very similar proof to that of Theorem 10. However, convolutional networks are notoriously more memory consuming and therefore computation of the robust upper bound requires more resources. We have then left this computation for future work, but we here report results for the other robust training methods using these more complex neural networks.

We evaluate a convolutional neural network (denoted as *CNN*) that has been commonly used in previous works of adversarial robustness Madry et al. (2019). It has two convolutional layers alternated with pooling operations, and two dense layers. We compare adversarial accuracy across four different methods: ARUB- $L_\infty$ , ARUB- $L_1$ , PGD- $L_\infty$  and Nominal training. Results for the CIFAR data set are shown in Table 15. We observe that the proposed methods ARUB- $L_1$  and ARUB- $L_\infty$  yield the highest adversarial accuracies with respect to PGD- $L_2$  attacks. For the MNIST data set and the FASHION MNIST data set (Table 16 and Table 17, respectively), we see that ARUB- $L_\infty$  has the highest adversarial accuracies with respect to PGD- $L_2$  attacks when  $\rho \leq 0.1$ , whereas PGD- $L_\infty$  does best for larger values of  $\rho$ .

$\rho =$	0.000	0.010	0.020	0.030	0.100	1.000	3.000	5.000	10.000
ARUB- $L_1$	71.17	70.98	70.70	70.51	<b>69.88</b>	<b>60.31</b>	<b>44.69</b>	<b>35.35</b>	<b>17.89</b>
ARUB- $L_\infty$	<b>72.03</b>	<b>71.76</b>	<b>71.45</b>	<b>71.25</b>	69.84	56.13	43.98	34.26	16.25
PGD- $L_\infty$	70.78	70.55	70.43	70.39	69.65	59.96	43.59	29.10	16.21
Nominal	71.29	71.13	71.05	70.66	69.38	48.16	16.05	10.04	10.04

Table 15: Adversarial Accuracy for CIFAR with CNN architecture and PGD- $L_2$  attacks.

$\rho =$	0.000	0.010	0.020	0.030	0.100	1.000	3.000	5.000	10.000
ARUB- $L_1$	91.25	91.09	90.78	90.55	89.02	82.46	68.95	54.80	33.20
ARUB- $L_\infty$	<b>91.37</b>	<b>91.13</b>	<b>91.05</b>	<b>90.86</b>	<b>90.59</b>	82.81	71.45	60.23	30.86
PGD- $L_\infty$	90.59	90.55	90.43	90.23	89.30	<b>84.45</b>	<b>73.20</b>	<b>67.54</b>	<b>57.77</b>
Nominal	91.02	90.90	90.62	90.43	89.02	77.85	56.72	40.51	10.16

Table 16: Adversarial Accuracy for Fashion MNIST with CNN architecture and PGD- $L_2$  attacks.

$\rho =$	0.000	0.010	0.020	0.030	0.100	1.000	3.000	5.000	10.000
ARUB- $L_1$	<b>99.38</b>	<b>99.38</b>	<b>99.38</b>	99.34	<b>99.30</b>	98.32	91.68	70.51	33.83
ARUB- $L_\infty$	<b>99.38</b>	<b>99.38</b>	<b>99.38</b>	<b>99.38</b>	<b>99.30</b>	<b>98.79</b>	95.70	87.46	47.93
PGD- $L_\infty$	99.22	99.22	99.14	99.14	99.02	98.55	<b>96.37</b>	<b>91.29</b>	<b>55.39</b>
Nominal	99.30	99.26	99.26	99.26	99.18	97.93	89.69	60.00	9.34

Table 17: Adversarial Accuracy for MNIST with CNN architecture and PGD- $L_2$  attacks.